

198-70

NATIONAL ADVISORY COMMITTEE FOR AERONAUTICS

# WARTIME REPORT

ORIGINALLY ISSUED

October 1945 as  
Memorandum Report L5I12

AN INVESTIGATION OF THE RANGER V-770-8 ENGINE

INSTALLATION FOR THE EDO XOSE-1 AIRPLANE

I - COOLING

By Robert N. Conway and M. Arnold Emmons, Jr.

Langley Memorial Aeronautical Laboratory  
Langley Field, Va.



WASHINGTON

3

**NACA WARTIME REPORTS** are reprints of papers originally issued to provide rapid distribution of advance research results to an authorized group requiring them for the war effort. They were previously held under a security status but are now unclassified. Some of these reports were not technically edited. All have been reproduced without change in order to expedite general distribution.

MR No. 15112

NATIONAL ADVISORY COMMITTEE FOR AERONAUTICS

MEMORANDUM REPORT

for the

Bureau of Aeronautics, Navy Department

AN INVESTIGATION OF THE RANGER V-770-8 ENGINE

INSTALLATION FOR THE EDO XCSE-1 AIRPLANE

I - COOLING

By Robert N. Conway and M. Arnold Emmons Jr.

SUMMARY

An investigation of the cowl and cooling of the Ranger V-770-8 engine installation in the Edo XCSE-1 airplane has been conducted in the Langley propeller-research tunnel. The present report contains engine temperature data and cooling correlation analyses of the engine and oil cooler. Three types of baffles were installed on the engine in the course of the tests: the Ranger conventional and turbulent-flow baffles, and the NACA-designed diffuser baffles.

Engine-cylinder cooling with either the conventional or turbulent-flow baffles is predicted (by the correlation method) to be adequate for military power with rich mixture, and cruise power with lean mixture, at the flight conditions selected for analysis. Oil cooling is predicted to be adequate at the selected conditions of military climb and maximum endurance cruise, and is shown to require a slightly larger flap exit area than was used in the test configuration for adequate cooling at military high speed.

Cylinder temperatures were below specified limits, but excessive temperatures were measured at the magneto and other locations on or about the engine.

The three baffle types were each of merit in cooling a different region on the cylinder. An optimum baffle design is thus indicated to combine the best features of the three tested.

## INTRODUCTION

At the request of the Bureau of Aeronautics, Navy Department, an investigation of the cowling and cooling characteristics of the power-plant installation for the Edo XOSE-1 airplane has been carried out in the Langley propeller-research tunnel. This airplane is a scout observation single-float seaplane powered with a Ranger V-770-8 engine. It has a design high speed with military power of approximately 192 miles per hour and a climbing speed of 108 miles per hour; maximum endurance in cruising flight is obtained at 90 miles per hour with 30 percent of normal power.

The wind-tunnel model was a full-scale mock-up of the forward part of the fuselage and the inboard sections of the wings. From the firewall forward, the engine and cowling installation duplicated that proposed for the prototype airplane.

The purpose of the investigation was to determine the aerodynamic and cooling characteristics of the engine installation from which the adequacy of cooling could be determined. A further purpose of the investigation was to ascertain the influence of several cowling and engine-baffle modifications on the aerodynamic and cooling characteristics. The aerodynamics of the cowling installation including drag, cooling-air flow, pressure distributions, and cooling pressure available data are presented and discussed in reference 1.

The present report contains the results of tests made to determine cooling correlation equations for two sets of baffles from which the pressure drops required for cooling the engine for several flight and power conditions are predicted and compared with those available to determine the adequacy of the engine cooling. In addition, results of measurements of heat rejection from the engine to the oil, and other oil cooler data are presented. From these the cooling-air pressure drops required for the same conditions used in the engine cooling predictions are predicted and compared with pressure drops available to determine if the oil cooler is adequate. Cylinder temperatures and other installation temperatures were measured under test conditions approximating sea-level climb at military power and maximum endurance cruise. After corrections to standard conditions had been made, the various installation temperatures were compared with limiting temperature values to

determine the adequacy of cooling of these installation parts. The individual cylinder temperature variations shown in these tests are comparable to sea-level flight results. Tunnel tests simulating normal power climb were made to evaluate the effect of the changes in baffles and cowlings modifications on engine installation temperatures. All data presented herein were obtained at tunnel airspeeds from 85 to 105 miles per hour.

#### APPARATUS

##### Model

The wind-tunnel model (fig. 1) was fabricated of metal and plywood to the scale of the actual airplane, duplicating the forward part of the fuselage and the inboard wing sections. The principal dimensions of the model are given in figure 2.

The cowlings, designed and constructed by the Ranger company, is discussed in detail in reference 1. This cowlings is similar to one developed previously at the Langley Laboratory for a similar engine in the Bell XP-77 airplane. Alternate arrangements and modifications of the cowlings, including shutter and flap-type cooling-air exits, were evaluated in power-off tests and reported in reference 1. The configuration used in the power-on tests of the present report and shown in figure 3 was based upon the results of the power-off tests. All cooling-air and charge-air required by the engine entered through the cowlings inlet to the pressure box. (See fig. 4.) Carburetor and oil-cooler air were then taken from the rear of the pressure box. Turning vanes were installed in the engine-cooling-air exits and in the oil-cooler inlet duct. The inlet and exit areas of the cowlings components are given in the following table:



The Ranger engine used in the model was operated from a control panel mounted outside of the test section of the tunnel. The installation of the engine in the model is shown in figure 5. Pertinent engine and propeller data are presented in the following table. Results of the type test and calibration of an engine of this series at the Naval Aircraft Factory are given in reference 2.

Impeller diameter, in . . . . . 7.625

Propeller . . . . .	Hamilton Standard (61C1A12) with molded blade root fairings
Type . . . . .	Constant speed
Number of blades . . . . .	2
Diameter, ft . . . . .	9

Three types of baffles were installed on the engine in the course of the tests. These are shown diagrammatically in figure 6. Conventional baffles currently in use on the V-770-6 and V-770-8 engines were installed on the outboard side of the cylinder barrels only as shown in figure 7. Turbulent-flow baffles, previously used in experimental installations of an earlier version of this engine, were installed on both the inboard and outboard sides of the cylinder heads and barrels. (See fig. 8.)

The turbulent-flow baffles were modified to permit adjustment of the space between the baffles on the cylinder barrels. A third baffle was designed and constructed at the Laboratory to cover only the cylinder barrels. (See fig. 9.) The diffuser exit of this baffle was designed to reduce exit losses encountered with the other types of baffles. The diffuser baffles were installed on the left bank only.

The arrangement of the oil-cooler installation is shown in figure 3. Some pertinent data on the oil cooler and oil-cooler system are given in the following table:

#### Oil-cooler duct

Inlet area, sq ft . . . . .	0.22
-----------------------------	------

Oil cooler . . . . .	UAP U-840713 - modified to pass all oil flow through the core
Shape . . . . .	Elliptical
Area, sq in. . . . .	74
Depth, in. . . . .	9
Tube, diameter, in. . . . .	9.21

A view of the rear face of the oil cooler is given in figure 10.

The flame damping exhaust stacks used at first (fig. 5) failed in operation as shown in figure 11. For the power-on tests, therefore, the fishtails were cut off as shown

in figures 1 and 3. Cooling-air shrouds were installed on the stacks as shown in figure 5.

### Instrumentation

Standard engine instruments included in the control panel were oil, fuel, and manifold pressure gages, oil-in thermometer, and engine tachometer. These were supplemented by numerous thermocouples, pressure tubes, and miscellaneous instruments installed at the Laboratory.

Cylinder temperatures were measured at the flange and in the spark-plug well, both inboard and outboard, and at outboard center of the cylinder barrel with imbedded thermocouples. Additional imbedded thermocouples were installed on cylinders 4-L and 4-R to obtain temperature variations over an entire cylinder. Gasket thermocouples were installed under each spark plug. Detailed location of the imbedded thermocouples is shown in figure-12. Iron-constantan wire was used in all thermocouples and all temperatures were recorded within  $\pm 3^{\circ}\text{F}$  by a Brown self-balancing potentiometer.

Cooling-air temperatures were measured with thermocouples installed at the cowl inlet and exits, in the engine vee, and in the accessory compartment. Shielded thermocouples were used in the engine vee (fig. 4) to minimize errors caused by radiation. Air temperatures in the wind stream and in the carburetor-air inlet were measured within  $\pm 1^{\circ}\text{F}$  on resistance thermometers. Oil temperatures into and out of the engine were measured with resistance thermometers (approximate error  $\pm 1^{\circ}\text{F}$ ).

Cooling-air pressures were measured with open-end tubes installed between the cylinder heads and in low-velocity regions behind the baffles as shown in figures 6, 7, 8, and 13. Oil-cooler air pressures were measured by open-end tubes extending through the cooler tubes to each face as shown in figure 10. Additional pressure measurements, discussed in reference 1, were made in the cowl inlet, cooling-air exits, carburetor deck, and other locations. All pressures were recorded from visual observation of a multitube manometer.

Fuel-air ratio was set approximately from a Cambridge fuel-air meter. Accurate determination was then made from fuel-flow measurements obtained with a rotameter and from

air-flow measurements obtained with a calibrated rectangular venturi installed in the charge-air inlet duct. The measurements of charge-air flow obtained with the venturi were found to agree within 4 percent with results from reference 2 for corresponding engine-operating conditions, differences in atmospheric conditions being considered.

The oil flow through the engine was measured with a calibrated orifice installed between the oil tank and the engine.

#### SYMBOLS

$c_p$	specific heat, Btu per pound per $^{\circ}\text{F}$
$D$	propeller diameter, feet.
$f/a$	fuel-air ratio
$H$	total pressure, inches of water
$K$	constant associated with correlation analysis
$m$	exponent associated with $(\sigma_a \Delta P_e)$
$n$	exponent associated with $W_p$
$P$	static pressure, inches of water
$\Delta P$	pressure drop = $H_f - P_r$ , inches of water
$q$	dynamic pressure = $\frac{1}{2} \rho V^2$ , Inches of water
$T$	effective thrust, pounds
$T_c$	thrust disk loading coefficient
$t$	temperature, $^{\circ}\text{F}$
$\Delta t_b$	charge-air temperature rise through blower, $^{\circ}\text{F}$
$t_g$	mean effective gas combustion temperature, $^{\circ}\text{F}$
$t_{g0}$	reference mean effective gas temperature, $^{\circ}\text{F}$

$t_{diff}$	difference between average oil and entering air temperature, °F
U	unit heat rejection, Btu per minute per 100° F
V	velocity; miles per hour
W	weight (rate of) flow, pounds per second
A	increment of
e	heat rejection, Btu per minute
$\eta$	propulsive efficiency
$\rho$	air density, slugs per cubic foot
$\sigma$	air density ratio, ( $\rho/0.002378$ )

#### Subscripts ,

a	air at stagnation conditions (upstream of engine)
c	oil-cooling air
e	engine-cooling air
f	upstream of oil cooler or engine
h	cylinder head
O	Navy air
oil	engine oil
P	engine charge air
r	downstream of oil cooler or engine
s	standard sea level

#### METHODS AND TESTS

Tests were conducted to enable prediction of anticipated cooling of the engine cylinders and oil in **flight** at sea level and at altitude, to evaluate cooling in

simulated sea-level flight, and to evaluate the effects of baffle and cylinder modifications on cooling. The configurations tested under power-on conditions and discussed in the present report are listed in the following table, together with the plotting symbols used in the presentation,

TABLE 1.- TEST CONFIGURATIONS

Configuration		Symbol	Distinctive engine and cowling components installed
II	c	$\triangle$	Conventional baffles Flapped exits Short exhaust stacks with shrouds Vaned oil-cooler-inlet duct
III	a	$\times$	Turbulent-flow baffles Flapped exits Short exhaust stacks with shrouds Vaned oil-cooler-inlet duct
	b		Baffle spacing varied on cylinder barrels
IV	a	$\diamond$	Diffuser baffles on left bank Turbulent-flow baffles on right bank Flapped exits Short exhaust stacks with shrouds Vaned oil-cooler-inlet duct
	b	+	<u>Short exhaust stacks without shrouds</u>
	e	$\nabla$	Short exhaust stacks without shrouds Flapped engine-cooling-air exits without vanes, firewall gap sealed

#### Prediction of Adequacy of Cooling in Flight

The adequacy of cooling of the engine cylinders and of the oil cooler for several engine and flight conditions was determined by comparing cooling-air pressure drops required for given temperature limits with the pressure-drops available. Correlation methods based on the wind-tunnel tests enabled prediction of the required cooling-air pressure drops. Available pressure drops were obtained

from wind-tunnel tests simulating flight conditions, as discussed in reference 1. The flight conditions selected for predictions of cooling adequacy are defined in the following table.

TABLE 2.- FLIGHT CONDITIONS FOR COOLING PREDICTIONS

	Military high speed		Military climb		Max. end. cruise
Altitude, ft	0	10,000	0	9,000	1500
Air temperature, °F	90	53	90	57	84
Speed, mph	191	203	108	122	90
Auto rich:					
f/a	0.104	0.102	0.104	0.103	-----
Charge air, lb/hr	4300	4300	4300	4300	-----
Auto lean:					
f/a	0.096	0.095	0.096	0.095	0.064
Charge air, lb/hr	4250	4250	4250	4250	970
Brake horsepower	550		550		153
Engine speed, rpm	3300		3300		1800
Spark plug temp, °F	518		518		464
Oil out temp, °F	220		220		220
Flap setting	Flush		Open		Flush
Flap area, sq ft					
Engine exit	0.44		1.69		0.44
Oil-cooler exit	.05		.41		.05

The increase in critical attitude over that of the engine specification results from carburetor ram, as discussed in reference 1.

Engine-cylinder cooling adequacy.- The engine-cylinder-cooling-correlation analysis was conducted for the two configurations employing the conventional baffles and the turbulent-flow baffles. Complete details of the method of analysis are presented in references 3, 4, and 5. This analysis leads to a relation between cylinder temperatures and engine and cooling conditions from which the cooling characteristics of an engine can be predicted with a minimum of testing. The relation is expressed as follows:

$$\frac{t_h - t_a}{t_g - t_h} = \frac{K(W_p)^n}{(\sigma_a \Delta P_e)^m} \quad (1)$$

where

$t_h$  average head temperature, °F (average of temperatures measured with thermocouples imbedded near the exhaust and intake spark plugs on all cylinders)

and the other quantities are as defined under Symbols.

The stagnation temperature was determined from the expression:

$$t_a = t_o + \frac{v_o^2}{2Jg c_p} \quad (2)$$

which reduces to

$$t_a = t_o + 1.79 \left( \frac{v_o}{100} \right)^2$$

The stagnation density ratio is expressed as:

$$\sigma_a = \frac{\rho_a}{\rho_s} = \frac{\rho_a}{0.002378} \quad (3)$$

where, from the gas laws,

$$\rho_a = \rho_o \left( \frac{t_a + 460}{t_o + 460} \right)^{\frac{1}{\gamma-1}} \quad (4)$$

From references 3, 4, and 5, it can be ascertained that

$$t_{g0} = t_{go} + \Delta t_g \quad (5)$$

The temperature  $t_{g0}$  is affected by fuel-air ratio, engine timing, and exhaust back pressure. For the present tests the engine timing was fixed and the back pressure change was small; thus these factors were neglected in determining the gas temperature.

The increment,  $\Delta t_g$ , is expressed as

$$\Delta t_g = 0.8 (t_{carb} + \Delta t_b) \quad (6)$$

where

$$t_{carb} = t_o + \Delta t_{carb} \quad (7)$$

(the increment  $\Delta t_{carb}$  being experimentally determined)



and

$$\Delta t_b = \frac{(\text{supercharger tip speed})^2}{J g c_p} \quad (8)$$

which reduces to

$$\Delta t_b = 14.4 \left( \frac{\text{engine speed, rpm}}{1000} \right)^2$$

Three series of tests, as outlined in the following table, were conducted to establish the relationship expressed in equation (1), and necessary auxiliary relationships. The tests were conducted with the model in the climb attitude at approximately 100 miles per hour.

To determine	Vary	Hold constant
m	$\Delta P_e$	$W_p$ , rpm, f/a pm, f/a
$t_{g_0}$ vs. f/a	f/a, rpm, $\Delta P_e$	

For the tests with constant fuel-air ratio, a value of  $\frac{f}{a} = 0.085$  was used.

The exponentials  $m$  and  $n$  were determined graphically from logarithmic plots and then utilized with the related data to plot equation (1) in the form

$$\frac{t_h - t_a}{t_g - t_h} \text{ vs. } \frac{W_p^{n/m}}{\sigma_a \Delta P_e}, \text{ whence the value of } K \text{ could be}$$

obtained. A value of  $t_{g_0} = 1070$  at  $\frac{f}{a} = 0.085$  was

found to correlate best as the required tie-point in the foregoing series of tests.

Data from the third series of tests were then substituted in the completed correlation equation in order to determine the variation of  $t_{g_0}$  with fuel-air ratio.

To utilize the correlation method of prediction, which is based on an average cylinder temperature, the relationship between the average temperature and the highest limiting cylinder temperatures was established.

The correlation equation may then be used to predict the average head temperature when the available cooling-air pressure drop, and all other engine and flight conditions are known. Finally, by using the established relationship of hottest versus average temperature, the peak cylinder temperature may be predicted.

Alternatively, the process may be reversed to predict the required pressure drop for a specified limiting temperature.

In either case, the available pressure drop is determined as a function of the propeller thrust disk-loading coefficient:

$$T_c = \frac{T}{\rho_o (1.467 V_o)^2 D^2} \quad (9)$$

The relationship between  $T_c$  and  $\sigma_a \Delta P_e$  (fig. 14) for the present model was determined during the wind-tunnel tests and is detailed in reference 1.

The thrust coefficient  $T_c$  used in the cooling prediction was obtained by correcting characteristics of a similar propeller to the activity factor, 99 per blade, of the present propeller, following standard propeller procedures. Using the approximate propulsive efficiencies of 85 percent in military high speed and 70 percent in military climb and maximum endurance cruise, the value of thrust used in the foregoing equation may be obtained within 3 percent from the equation

$$T = \frac{375 \eta_{bhp}}{V_o} \quad (10)$$

where the value of brake horsepower  $bhp$  is that given in table 2.

Oil-cooling adequacy.— The oil-cooling correlation analysis required determining the characteristics of the engine-oil system as a function of engine revolutions per minute, and determining the unit heat rejection and cooling-air pressure drop of the oil-cooling system as a function of cooling-air flow. This information was obtained in tests simulating maximum endurance cruise, 60 percent power climb, normal power and military power climb, approximately, and other tests necessary to cover the required range. In each of

these tests the engine was operated at steady conditions and of?, temperatures were stabilized. Inlet conditions were not controlled, the oil-in temperature varying from 157° F to 214° F, and the air-in temperature varying from 100° F to 125° F.

The unit heat rejection is defined as the oil heat rejection per 100° F difference between the average oil temperature and the air-in temperature.

$$U = \frac{\theta_{oil}}{t_{diff}/100}, \text{ Btu}/100^\circ \text{ F}/\text{min} \quad (11)$$

where

$$t_{diff} = \frac{t_{oil \text{ out}} + t_{oil \text{ in}}}{2} - (t_a + 5) \quad (12)$$

it having been determined experimentally that the entering air temperature was approximately 5° higher than the stagnation temperature.

6s in the engine-cooling correlation analysis, it is possible to predict; either the limiting (oil out) temperature or the required cooling:-air pressure drop. To determine the required pressure drop, the engine-oil system characteristics are read as a function of engine revolutions per minute and then used to compute the unit heat rejection for which the required cooling-air flow may be read. The uncorrected required cooling-zfr pressure drop, based on the density ratio at the rear of the cooler, may then be read. To correct for the addition of heat to the air, the density ratio at the rear of the oil cooler is evaluated by utilizing the pressure at the front of the cooler, the approximate pressure drop through the cooler, and the oil-heat rejection characteristics. The equations used in this step are:

$$\sigma_r = \frac{H_r}{(460 + t_r)} \times \frac{(460 + t_s)}{p_s} \quad (13)$$

or

$$\sigma_r = 1.27 \frac{H_r}{(460 + t_r)}$$

where

$$H_r \approx H_f - \Delta P_c \quad (14)$$

$$\Delta P_c \approx \frac{\sigma_r \Delta P_c}{\sigma_a} \quad (15)$$

and

$$t_r = (t_a + 5) + \frac{\theta_{oil}}{(0.24 \times W_c)} \quad (1.6)$$

The variation of front pressure  $H_f$  with  $T_c$  is shown in figure 15, and the available pressure drop,  $\Delta P_c$ , is shown in figure 16. These two curves are discussed further in reference 1.

#### Measurement of Cooling in Simulated

##### Flight at Sea Level

The cruising and climbing speeds of the XCSE-1 are such that it was possible to approximate closely the conditions of maximum endurance cruise and military power climbing flight in the wind tunnel. Accordingly, temperatures of the entire engine installation were obtained under these conditions for the cowl and baffle configuration (IIC) to be installed on the prototype airplane. Corrections to a free air temperature of 90°F (Navy standard) were made as specified in reference 6, and the temperatures then compared with limiting temperatures specified in references 6 and 7. Limitations of the wind-tunnel-speed control prevented exact duplication of flight speeds in these tests. The maximum attainable horsepower was approximately 525 brake horsepower, being limited by the venturi installation in the charge air intakes. Fuel-air ratios were inadvertently set richer than specified. Despite these deviations from specified flight conditions, the accessory temperatures are considered to be representative of those that would be encountered at the specified flight conditions. By means of the correlation analysis, peak cylinder temperatures are readily predictable for the specified conditions.

The method of temperature correction is based on a correction empirically determined to be directly proportional to the difference in measured and specified free air temperature. No temperature corrections were applied for the difference between test and standard-air cooling-air pressure drops, inasmuch as calculations showed such corrections to be negligible.

This test information enables prediction of accessory temperatures not predictable by any more rigorous method yet developed. Inasmuch as these test conditions closely approximate sea-level flight conditions, the individual cylinder temperature variations from the average are comparable to these which would be experienced in flight. In addition, a comparison with correlation-predicted temperatures may be made.

#### Evaluation of Baffle and Cowling Modifications

In order to evaluate the effects on engine-cylinder and other engine-installation temperatures of different cylinder baffles, tests of three baffle types were conducted at the normal power climb condition, approximately. The conventional engine baffles, the turbulent-flow baffles, and the diffuser baffles were tested. As indicated in the configuration table, the diffuser baffles were installed on the left bank only, the turbulent-flow baffles being installed on the right bank for this configuration. The test conditions are noted in the following table:

Flight condition: Normal power climb, approximately			
Configuration	Baffles	Inlet air (°F)	f/a
IIc	Conventional	112	0.086
IIIA	Turbulent flow	110	.098
IVa	Diffuser, turbulent flow	107	.098

In the presentation, the results have been corrected by the method of reference 6 to a common inlet air temperature of 90° F. The cylinder temperature of configuration IIc has been further corrected to a fuel-air ratio of 0.098 by use of the relation  $\frac{t_h - t_a}{t_g - t_h} = \text{a constant}$  which follows from the engine-cooling correlation.

The effects on cylinder temperatures of varying the baffle spacing on the cylinder barrels were evaluated with the turbulent-flow baffles on all cylinders (configuration IIIB) at a test condition approximating 90 percent power climb. The presented results have been corrected to a common inlet air temperature and a common fuel-air ratio,

A brief series of tests evaluating the effects on engine temperature of some cowling modifications was made at approximately normal power climb condition. The test conditions are indicated in the following table.

Configuration	Modification	Inlet air (°F)	f/a
IVa	None - basis of comparison	107	0.098
IVb	Exhaust stack shrouds removed	108	.098
IVc	Exhaust stack shrouds removed, engine-cooling-air exit vanes removed, and cowl-firewall gap sealed.	116	.100

In the presentation, the results were corrected to a common inlet-air temperature and fuel-air ratio.

## RESULTS AND DISCUSSION

Results are presented to show the adequacy of engine-cylinder cooling and of oil-cooling as predicted by the cooling correlation analyses. In addition, individual cylinder temperatures and other installation temperatures measured under conditions comparable to sea-level flight conditions are presented. An evaluation of the effects on engine temperatures of baffle and cowling modifications is also shown, as discussed under Methods and Tests.

### Predicted Cooling in Flight

The predicted adequacy of cooling in flight is based upon the methods and tests discussed in the preceding section. The working charts are presented on which the correlation analyses are based, and the additional charts necessary to use the analyses are shown.

Engine-cylinder-cooling correlation.- The variation of the differential temperature ratio with  $W_p$  and  $\sigma_a \Delta P_e$  is shown in figures 17 and 18, respectively, for the conventional and turbulent-flow baffle installations. Substitution of the values of  $m$  and  $n$  determined from

these plots enables preparation of the completed analysis curves in figure 19 whence the correlation equations were obtained as

(a) Configuration IIc

$$\frac{t_h - t_a}{t_g - t_h} = 0.89 \left( \frac{W_p^{2.00}}{\sigma_a \Delta P_e} \right)^{0.27}$$

(b) Configuration IIIa

$$\frac{t_h - t_a}{t_g - t_h} = 1.21 \left( \frac{W_p^{1.66}}{\sigma_a \Delta P_e} \right)^{0.40}$$

The correlation for the turbulent-flow baffles differs from that obtained in a previous investigation for a somewhat similar configuration. This difference is attributed to changes in the carburetion, in the blower, and in the baffle design.

The variation of reference mean effective gas temperature with fuel-air ratio is shown in figure 20. It was possible to fair a common curve through the points obtained for both configurations. In obtaining this curve, a carburetor temperature rise of 70°, experimentally determined, was used in equation (7).

The relation between hottest and average cylinder temperatures, necessary in applying the condition, is presented in figure 21. It has been noted that the value of  $t_h$  used in the present correlation is based on the average of temperatures measured with thermocouples imbedded near the exhaust and intake spark plugs. This is in accordance with recent practice directed toward standardization of procedures. The relationship between average imbedded cylinder head temperatures and the average spark plug gasket temperatures as used in earlier correlation work is shown in figure 22.

Predicted adequacy of engine-cylinder cooling. - A comparison of the required engine-cooling-air pressure drop, predicted by the correlation method, with the available pressure drop is presented in the following table, for the flight conditions specified in table 2.

TABLE III.- ADEQUACY OF ENGINE-CYLINDER COOLING

	Flight condition	Altitude (ft)	Speed (mph)	$\Delta P_e$ (in. H <sub>2</sub> O)		
				Required auto rich	Required auto lean	Available
Conventional baffles Configuration IIc	Military high speed	0 5,000	191 203	6.6 5.9	9.0 8.1	11.5 10.0
	Military climb	0 9,000	108 122	6.4 5.7	8.8 8.1	9.0 8.6
	Max. endurance cruise	1,500	90	---	.9	3.4
Turbulent-flow baffles Configuration IIIa	Military high speed	0 10,000	191 203	7.8 8.0	10.1 10.0	11.5 10.0
	Military climb	0 9,000	108 122	7.7 7.8	10.0 9.9	9.0 8.6
	Max. endurance cruise	1,500	90	---	1.4	3.4

NATIONAL ADVISORY  
COMMITTEE FOR AERONAUTICS



A sample calculation is shown in Appendix A.

The available pressure drop is adequate for each of the specified flight conditions with the mixture set at automatic rich. With the exception of the turbulent-flow baffle installation in military climb, the available pressure drop is also adequate for the specified flight conditions with the mixture set at automatic lean.

The selection of exit areas and flap settings to furnish a required pressure drop is discussed in reference 1, together with a presentation of cowling design charts. It is apparent that, with the mixture at automatic rich, the cowl flaps may be partially closed thereby reducing the drag and permitting higher flight speeds. Alternatively, the mixture may be set at automatic lean and the fuel consumption decreased for high power operation at the expense of a larger cowling drag.

oil-cooling correlation. The characteristics of the engine lubrication system as a function of engine revolutions per minute are shown in figure 23. The heat rejection from the engine to the oil, the oil temperature rise across the engine, the rate of oil flow and oil pressure are shown. To indicate the engine horsepower of the tests, a curve of manifold pressure is also shown. A maximum oil-heat rejection of 2100 Btu per minute was measured at 3300 revolutions per minute, at an oil flow of 105 pounds per minute and a temperature difference of  $36^{\circ}$  F between oil out of the engine and oil into the engine. No effect of baffle configuration was noted in these tests.

The unit heat rejection of the oil cooler as a function of oil-cooler air flow is shown in figure 24. In addition the variation of the cooling-air pressure drop across the cooler is shown as a function of cooling-air flow.

Predicted adequacy of oil cooling. The required oil-cooling-air pressure drop, predicted by the correlation method for the flight condition specified in table 2, is compared in the following table with the available pressure drop.

TABLE 4.- ADEQUACY OF OIL COOLING

Flight condition	Altitude (ft)	Speed (mph)	$\Delta P_c$ (in. H <sub>2</sub> O)	
			Required	Available
Military high speed	0	191	8.9	4.1
	10,000	203	6.1	3.5
Military climb	0	108	7.9	11.0
	9,000	122	6.1	10.5
Max. endurance cruise	1,500	90	0.6	1.3

A sample calculation is shown in Appendix B.

The available pressure drop is adequate for satisfactory oil cooling in military climb and in maximum endurance cruising flight. Adequate pressure drop may be obtained in military high speed by increasing the flap opening. From the cowling design charts of reference 1, it is determined that increasing the exit area (flap flush) to 0.10 square feet would provide the required pressure drop.

#### Measured Cooling in Simulated Flight at Sea Level

Engine cylinder temperatures measured during tests approximating military power climb and cruising flight conditions are shown in figure 25, and corresponding installation temperatures are given in table 5, part (a). These temperatures have been corrected to an inlet air temperature of 90°, and in table 5, the correction factors used are tabulated. Cylinder temperatures were corrected by a factor of 1.0 on the heads and 0.7 on the flanges.

Temperature limits, with which these results may be compared, are listed in the following tables:

#### Cylinder-Temperature Limits

Power rating	Spark plug gasket temperature (°F)	Flange temperature (°F)
Military, 550 bhp	518	315
Normal, 500 bhp - hr	518	315
Cruise, 350 bhp and below	464	302

## Installation-Temperature Limits

Item	Temperature (°F)
Oil in, minimum temperature	145
Oil out, maximum	220
Spark-plug elbow	250
Magneto	155
Accessory compartment	140
Carburetor rise	9

The specified limits were exceeded in the accessory compartment at the cruising condition, and on the magneto at both the cruising and climbing conditions. The carburetor air temperature did not exceed the limit.

The pattern of engine-cylinder variation was generally unaffected by the engine power condition. Engine cylinder temperatures nowhere exceeded the specified limits, inasmuch as the test fuel-air ratios were extremely rich. However, in the previous prediction of cooling adequacy it is indicated that satisfactory engine-cylinder cooling will be experienced at specified values of fuel-air ratio. A comparison of these data with calculations using the correlation method at the conditions of test, indicated an agreement within 4°F of the average head temperature in maximum endurance cruise, and within 7°F in military power climb.

## Effects of Baffle and Cowling Modifications

Evaluation of baffle type.— The relative merits of the various types of engine baffles are shown by the average temperatures measured at corresponding points on the various cylinders (fig. 26). These data show that the spark-plug temperatures were lower with the turbulent-flow baffles than with either of the other designs, whereas flange temperatures with conventional baffles were below those with the turbulent-flow or diffuser baffles. The lowest barrel temperatures were obtained with the diffuser installation designed at the Laboratory. A more detailed comparison of the cylinder temperature with the various baffle configurations is presented in figure 27. The pattern of temperature variation over the engine was generally unaffected by changes in baffle configuration (fig. 27(a)).

Temperatures measured at 17 points on cylinder 4-L and 4-R with each baffle configuration are shown in figure 27(b). An inspection of the temperatures measured on cylinder 4-L, as shown in figure 27(b), indicates that the lowest average temperature over the entire cylinder barrel was obtained with the diffuser baffle. This baffle appears to be deficient only at the flange and outboard spark-plug thermocouple locations. It is apparent that modification of the diffuser baffle at the flange would result in improved cooling at this location. The feasibility of this modification is shown in the baffle drawing, figure 6. Application of the diffuser design to a head baffle would be expected to reduce the temperature at the outboard spark plug.

Other installation temperatures (table 5, part (b)) recorded during the tests with the various baffles show that the recommended limits were exceeded on the magneto by  $33^{\circ}$  to  $43^{\circ}$  and on the spark-plug elbows of cylinder 4-R by  $20^{\circ}$  to  $35^{\circ}$  for each installation, and under some conditions on the plug elbows of cylinder 1-R. Carburetor air temperature was marginal.

Evaluation of various spacings of the turbulent-flow baffles on the cylinder barrels.- Temperatures recorded during the series of tests made to evaluate baffle-gap effects are shown in figure 28. To expedite testing, the spacings were different on the various cylinders during each test. It is believed that the error introduced because of varied spacings is of secondary importance.

The cylinder temperature as a function of outboard and inboard gap is shown in figure 29(a) and (b), respectively. These data indicate that the outboard gap should be set between  $\frac{3}{4}$  and 1 inch on both banks. Inboard gap settings of approximately  $2\frac{1}{2}$  inches on the Left bank and  $1\frac{3}{4}$  inches on the right bank appear to provide the lowest temperatures. In general, the inboard gap setting appears to be less critical than the outboard setting. As the outboard gap area is reduced below the effective free area between cylinders, a rapid increase in temperature may be expected.

The standard settings, used in all other tests of these baffles were  $\frac{1}{2}$  inch on the outboard side of both

banks,  $2\frac{3}{4}$  inches on the left bank inboard, and  $1\frac{1}{2}$  inches on the right bank inboard,

Effect of removing exhaust-stack shrouds.- The effect on engine temperatures of removing the exhaust-stack shrouds is shown in figure 30 and table 5. Inboard cylinder head temperatures were slightly higher without the shrouds, but the outboard head temperatures were reduced because of the increased cooling air flow.

Although changes in cylinder temperatures were small, appreciable increases in other installation temperatures accompanied removal of the shrouds, (see table 5, part (c)). The carburetor air temperature was increased to  $14^{\circ}\text{F}$  above the free-stream temperature, the spark-plug elbows were hotter and the accessory compartment temperature was increased to  $35^{\circ}\text{F}$  above the free-stream temperature.

Effect of removing the engine-air exit vanes and sealing the firewall gap.- Simultaneous sealing of the firewall-cowling gap and removal of the engine-cooling-air exit vanes are shown in figure 31 to have had negligible influence on the engine cylinder temperatures. This change, however, by reducing the flow through the accessory compartment effected a  $15^{\circ}\text{F}$  rise in accessory compartment temperature. (See table 5, part (c).)

#### CONCLUDING REMARKS

The principal results of the tests of the XOSE-1 power plant installation, as discussed in the present report, may be summarized briefly:

1. Engine-cylinder cooling with the conventional baffles is predicted to be adequate (by the correlation method) for the military power and cruise power flight conditions selected for analysis.
2. Engine-cylinder cooling with the turbulent-flow baffles is predicted to be adequate for the selected flight conditions, except in military climb at an auto lean mixture setting. If operation in the auto lean condition is desired, adequate cooling may be obtained with larger exit areas.
3. Oil cooling is predicted to be adequate (by correlation method) for the selected flight conditions of military climb and maximum endurance cruise, but inadequate in

military high speed. However, adequate cooling may be obtained in military high speed by increasing slightly the exit area.

4. Specified temperature limits were exceeded in the accessory compartment and at the magneto in tests approximating the maximum endurance cruise condition, and at the magneto in normal and military power climb conditions with the conventional baffle installation. Magneto temperatures were also excessive with the other two baffle installations under test conditions approximating normal power climb. Excessive spark-plug elbow temperatures were encountered under test conditions approximating normal power climb with all three baffle types.

5. The conventional baffles were found to provide lower peak flange temperatures, the turbulent-flow baffles provided lower peak head temperatures, and the NACA designed diffuser baffles provided lower cylinder barrel temperatures. Incorporation of the best features of the three types into one baffle, which appears to be feasible, would be expected to provide improvements in cylinder cooling.

6. Optimum spacing between turbulent-flow baffles, on the barrels, was found to be approximately 1 inch on the outboard side of both banks,  $2\frac{1}{2}$  inches on the left bank inboard side, and  $1\frac{3}{4}$  inches on the right bank inboard side.

7. Removal of the exhaust-stack shrouds affected cylinder temperatures only slightly, but increased the carburetor air temperature above the specified limit, as well as increasing spark-plug elbow temperatures and the accessory compartment temperature.

8. Simultaneous sealing of the firewall-cowling gap and removal of the engine-cooling-air exit vanes had

little effect on cylinder temperatures but increased the accessory compartment temperature.

Langley Memorial Aeronautical Laboratory  
National Advisory Committee for Aeronautics  
Langley Field, Va.

## APPENDIX A

## CALCULATION OF ADEQUACY OF ENGINE-CYLINDER COOLING

The procedure followed in determining the engine-cooling-air pressure drop required and the available pressure drop is shown in the following table, applying to the conventional baffle installation in military high speed at sea level.

	Item	Source	
1.	Engine-cooling-air flap setting		Flush
2.	True airspeed, $V_o$ , mph		191
3.	Altitude, ft		0
4.	Air temperature, $t_o$ , °F		90
5.	Air density, $\rho_o$ , slugs/cu ft	Specified	0.002248
6.	Brake horsepower		550
7.	Engine rpm		3300
8.	Fuel-air ratio (auto lean)		0.096
9.	Temperature limit of hottest head, °F		518



	Item	Source	
10.	Dynamic pressure, $q_o$ , in. water	Items 2, 5	16.97
11.	Cooling-air temperature, $t_a$ , °F	2, 4, eq.(2)	97
12.	Cooling-air density ratio, $\sigma_a$	4, 5, 11, eq.(3),(4)	0.976
13.	Average head temperature, $t_h$ , °F	9, fig. 21(a)	478
14.	Reference gas temperature, $t_{go}$ , °F	8, fig. 20	980
15.	Gas temperature increment, $\Delta t_g$ , °F	4, 7, eq. (6),(7),(8)	203
16.	Mean effective gas temperature, $t_g$ , °F	14, 15, eq. (5)	1183
17.	Temperature difference ratio $(t_h - t_a)/(t_g - t_h)$	11, 13, 16	.540
18.	$(W_p)^{n/m}/\sigma_a \Delta P_e$	17, fig. 19	.157
19.	Charge-air flow, $3600 W_p$ , lb/hr	6, 7, ref. 2	4250
20.	$(W_p)^{2.00}$	19	1.392
21.	$\sigma_a \Delta P_e$ , in. water	18, 20	8.82
22.	Required pressure drop, $\Delta P_e$ , in. water	12, 21	9.0
23.	$T_c$	Eq. (9)	.064
24.	Available pressure ratio, $\Delta P_e/q_o$	1, 23, fig. 14	.68
25.	Available pressure drop, $AP$ , in. water.	10, 24	11.5

## APPENDIX B

## CALCULATION OF ADEQUACY OF OIL-COOLING

The procedure followed in determining the oil-cooler-air pressure drop required for military high speed at sea level and the pressure drop available is shown in the following table.

1.	Oil-cooler flap setting		Flush
2.	True airspeed, $V$ , mph		191
3.	Altitude, ft		0
	Air temperature, $t_o$ , °F		90
4.			
5.	Air density, $\rho_o$ , slugs/cu ft	Specified	0.002248
6.	Air pressure, $p_o$ , in. water		408
7.	Brake horsepower		550
8.	Engine rpm		3300
9.	$t_{oil}$ out, °F		220

	Item	Source	
10	Dynamic pressure $q_o$ , in. water	Items 2, 5	16.97
11	Cooling-air temperature, $t_a$ , °F	2, 4, eq. (2)	97
12	Cooling-air density ratio, $\sigma_a$	4, 5, 11, eq. (3), (4)	0.976
13	Oil temperature rise, $\Delta t_{oil}$ , °F	8, fig. 23	36.0
14	Oil flow, $W_{oil}$ , lb/min	8, fig. 23	104.0
15	Oil heat rejection, $q_{oil}$ , Btu/min	8, fig. 23	2100
16	$t_{oil}$ , in	9, 13	184
17	$t_{diff}$ , °F	9, 11, 16, eq. (12)	105
18	Unit heat rejection, $U$ Btu/min/100° F	15, 17, eq. (11)	2000
19	Oil-cooler air flow, $W_c$ , lb/min	18, fig. 24	216
20	$\sigma_r \Delta P_c$ , in. water	19, fig. 24	7.9
21	$T_c$	eq. (9)	0.064
22	$(H_f - p_o)/q_o$	1, 21, fig. 15	1.28
23	$H_f$ , in. water	5, 10, 22	430
24	$H_r$ , in. water	12, 20, 23, eq. (14), (15)	422
25	$t_r$ , °F	11, 15, 19, eq. (16)	143
26	$\sigma_r$	24, 25, eq. (13)	.89
27	$\Delta P_c$ , required., in. water	20, 26	8.9
28	$\Delta P_c/q_o$ available	1, 21, fig. 16	.24
29	$\Delta P_c$ available, in. water	10, 29	4.1

## REFERENCES

1. Nichols, Mark R., and Dennard, John S.: An Investigation of the Ranger V-770-8 Engine Installation for the Edo XCSE-1 Airplane. II - Aerodynamics. NACA MR No. L5112b, 1945.
2. Atkinson, A. S., and Dahle, D. E.: Calibration of Ranger V-770-8 Engine. TED No. NAM-0434, NAES, Philadelphia Navy Yard, Bur. Aero., Navy Dept., April 20, 1944.
3. Pinkel, Benjamin: Heat-Transfer Processes in Air-Cooled Engine Cylinders. NACA Rep. No. 612, 1938.
4. Pinkel, Benjamin, and Ellerbrock, Herman H., Jr.: Correlation of Cooling Data from an Air-Cooled Cylinder and Several Multicylinder Engines. NACA Rep. No. 683, 1940.
5. Schey, Oscar W., Pinkel, Benjamin, and Ellerbrock, Herman H., Jr.: Correction of Temperatures of Air-Cooled Engine Cylinders for Variation in Engine and Cooling Conditions. NACA Rep. No. 645, 1938.
6. Anon.: Specification for the Measurement of Engine Installation Temperatures, NAVAER E-59c, Bur. Aero., July 7, 1943.
7. anon.: Model Specification - Engine, Aircraft; V-770-8, Ranger Aircraft Engines, SGV-770C-2. Specification No. 162-B, Ranger Aircraft Engines, Nov. 5, 1941, Rev. Jan. 31, 1944.

TABLE 5.- ENGINE ACCESSORY TEMPERATURES

Test condition	(a)Temp. of design installation		(b)Barfle change				(c)Installation change			
	IIc	IIc	IIc	IIc	IIc	IIc	IIc	IIc	IIc	IIc
Configuration	1800	3280	3150	3150	3150	3150	3150	3150	3150	3150
RPM	153	525	500	500	500	500	500	500	500	500
BHP	.084	.124	.086	.098	.098	.098	.098	.098	.098	.100
Fuel-air ratio	flush	open	open	open	open	open	open	open	open	open
Flap setting	88	104	104	104	104	104	104	104	104	104
Airspeed, mph										
Temperatures - °F										
As measured	100	117	112	110	107	108	116			
Free stream air										
Inlet air	90	90	90	90	90	90	90	90	90	90
Carburetor air	99	95	100	97	96	104	104	104	104	104
Air in vee	96	95	97	97	97	101	101	101	101	100
Engine-cooling-exit air, left	153	143	144	159	181	194	194	194	194	173
Engine-cooling-exit air, right	157	144	133	153	121	160	160	160	160	151
Inlet air	92	92	94	95	95	99	99	99	99	97
Exit air	139	137	138	145	143	148	148	148	148	142
Oil in	182	186	183	186	191	202	202	202	202	199
Oil out	---	218	---	229	222	233	233	233	233	230
Engine case, right side	192	217	223	232	229	236	236	236	236	234
Engine mount, right side	143	138	145	156	---	175	175	175	175	172
Magneto	179	189	188	197	198	181	181	181	181	202
Accessory compartment	146	111	109	108	110	125	125	125	125	140
Sparkplug elbow, 1-R intake	213	197	236	257	265	268	268	268	268	268
Sparkplug elbow, 2-L exhaust	---	---	---	115	116	---	---	---	---	134
Sparkplug elbow, 3-L exhaust	108	109	117	113	115	128	128	128	128	125
Sparkplug elbow, 4-L intake	109	109	114	111	109	125	125	125	125	124
Sparkplug elbow, 4-R intake	229	231	270	276	285	289	289	289	289	289
Sparkplug elbow, 4-R exhaust	117	119	130	128	132	145	145	145	145	142
Sparkplug elbow, 5-R intake	137	136	149	173	174	177	177	177	177	176
Sparkplug elbow, 6-L intake	197	191	223	206	217	217	217	217	217	217

\* As specified in reference 6

1 Average

NATIONAL ADVISORY  
COMMITTEE FOR AERONAUTICS

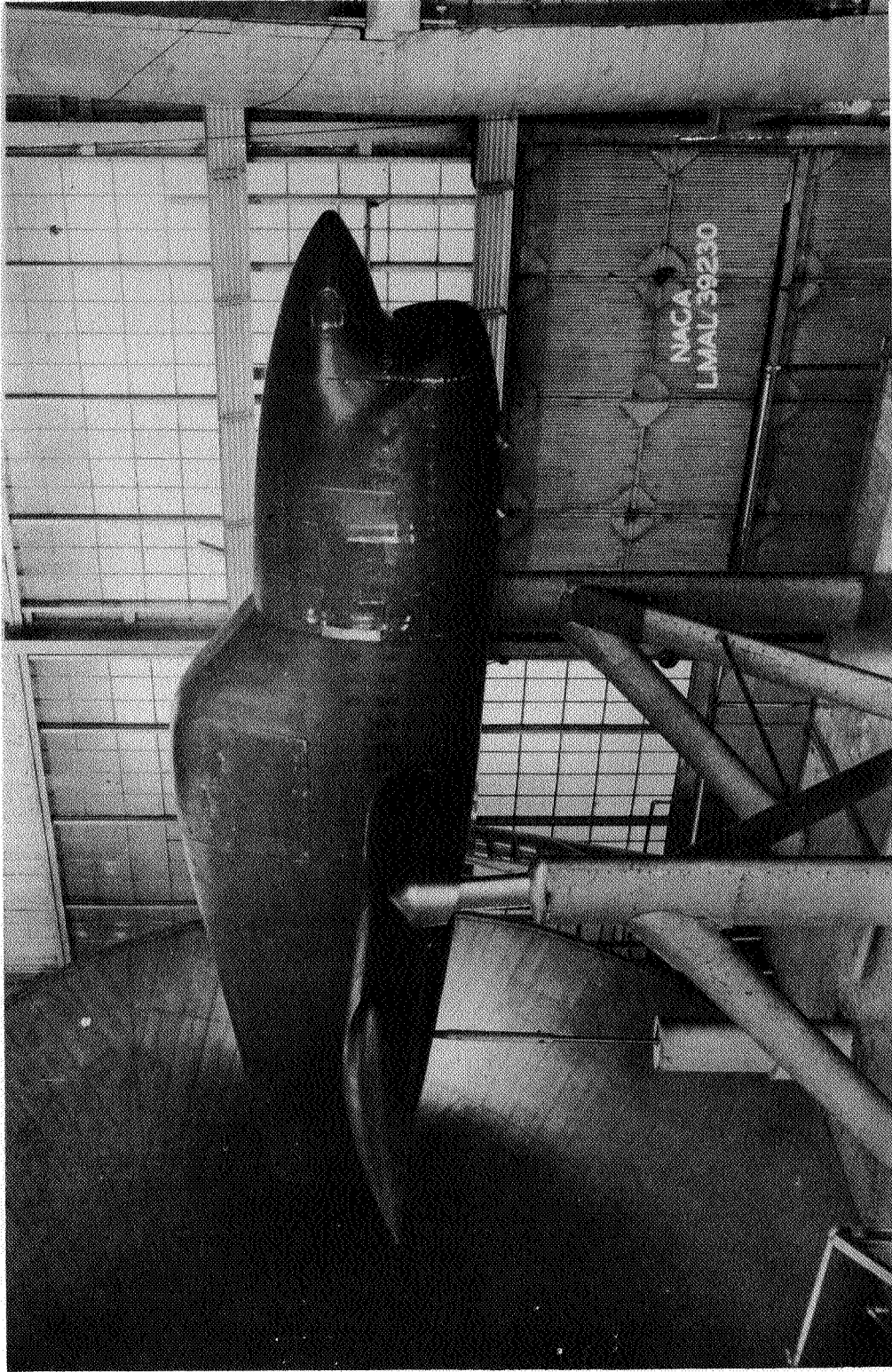
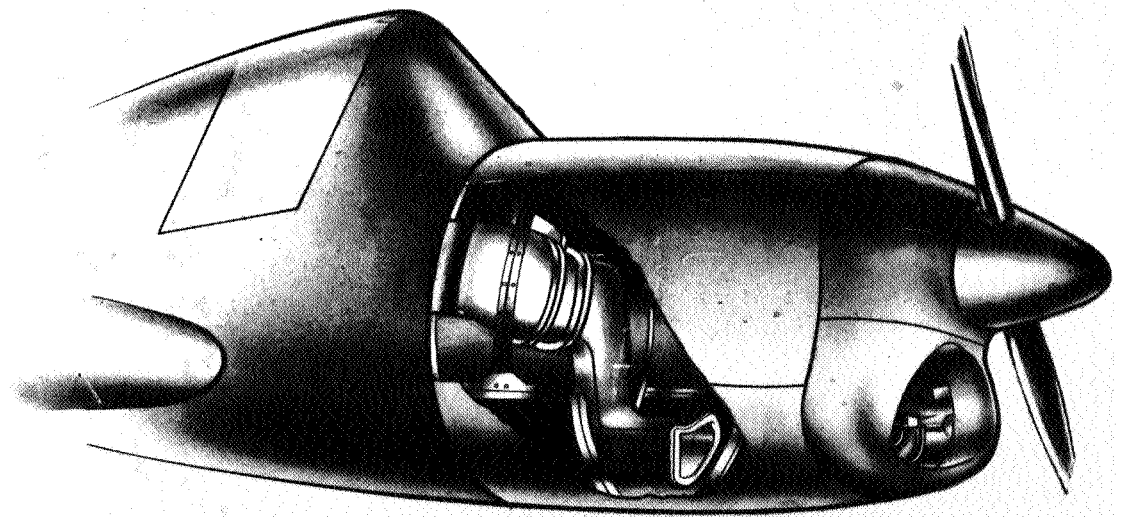
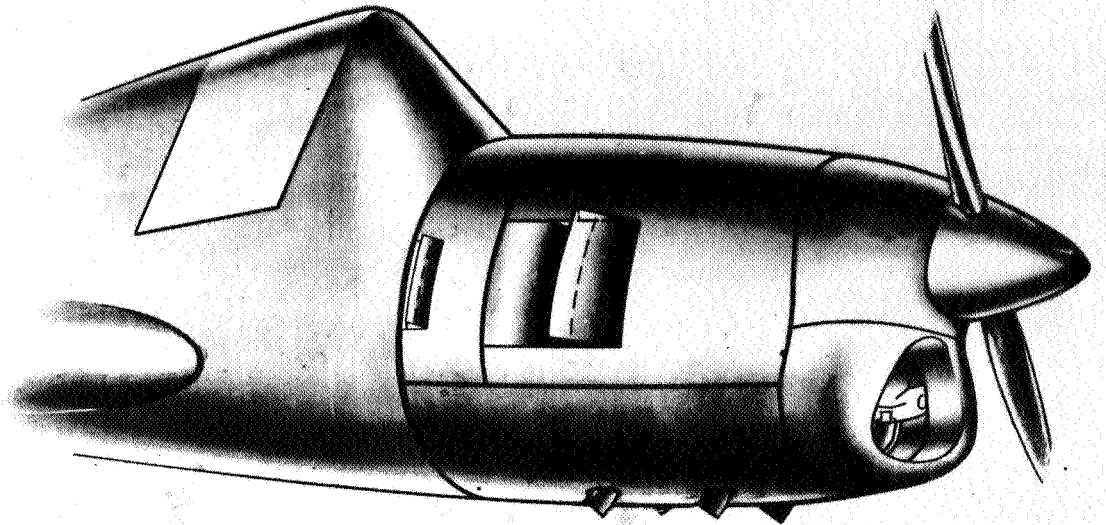


Figure 1.- XOSE-1 mock-up installed in tunnel.



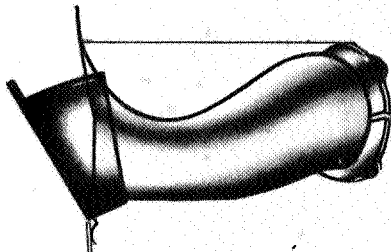
Figure 2 . - General arrangement and principal dimensions of model.

L-561

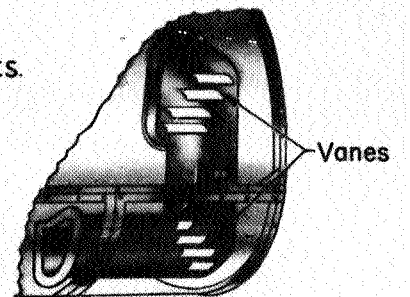


Oil cooler installation

NATIONAL ADVISORY  
COMMITTEE FOR AERONAUTICS.



Oil cooler exit duct



Oil cooler inlet duct

FIGURE 3.- COWLING DETAILS



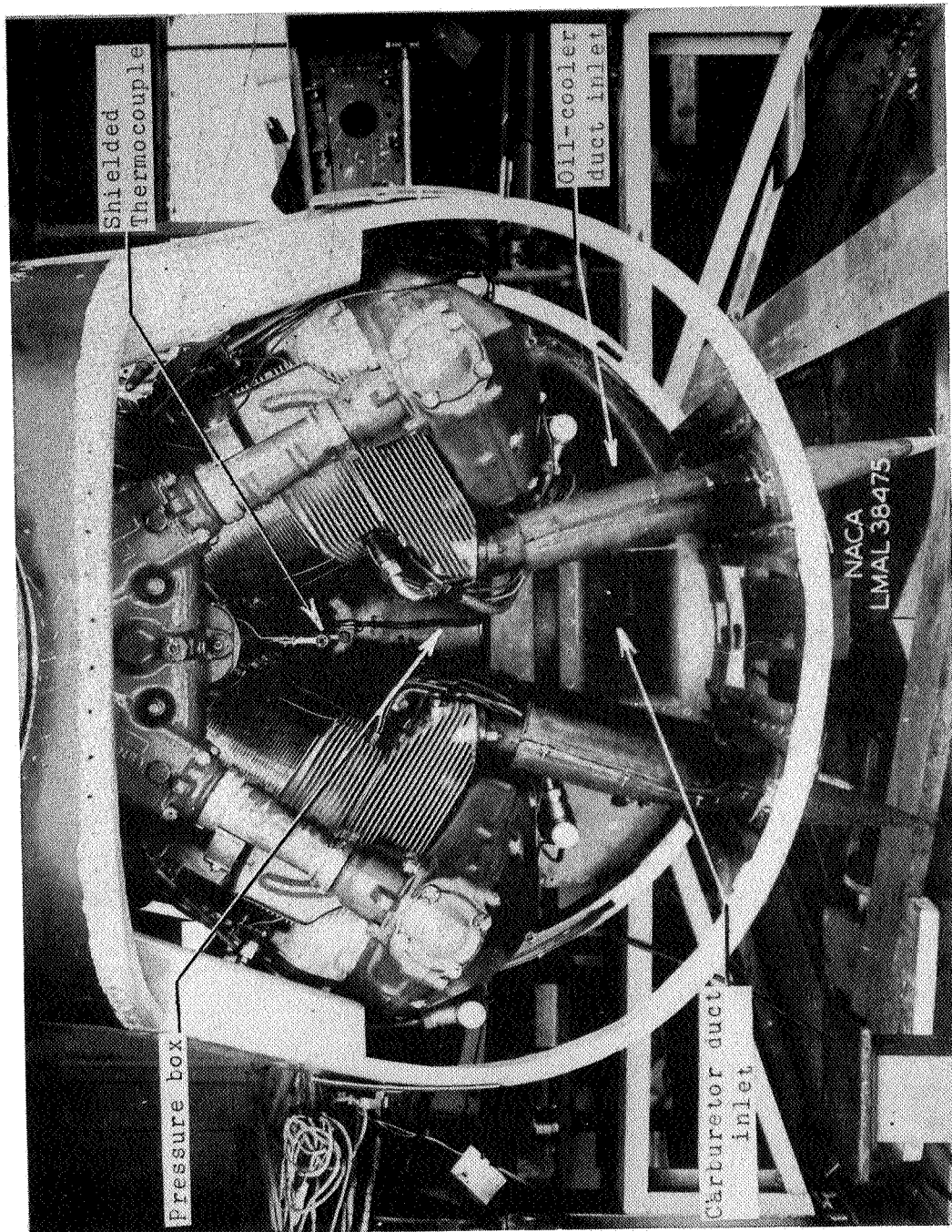


Figure 4.- Duct inlets and pressure box.

MR No. L5I12

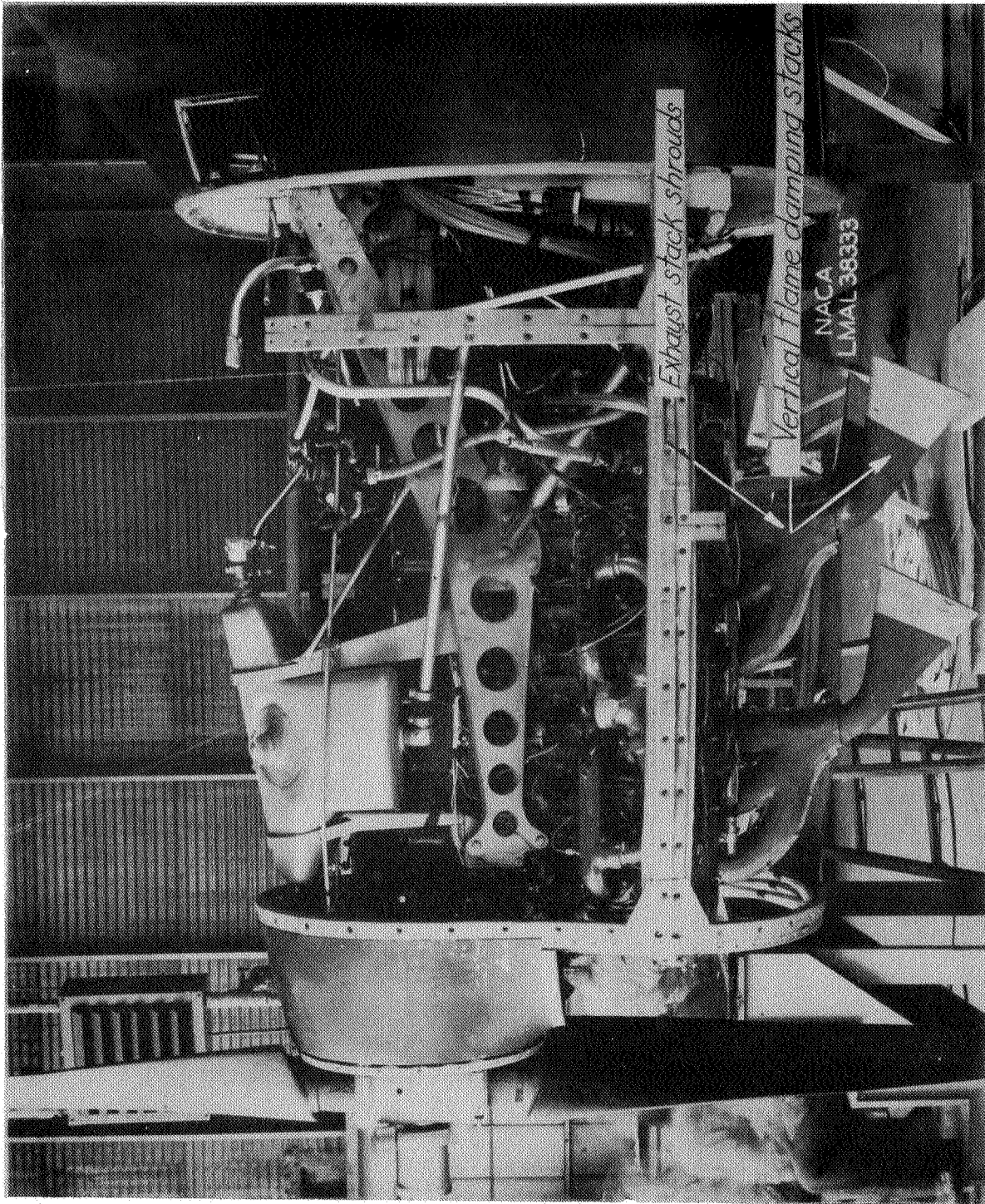
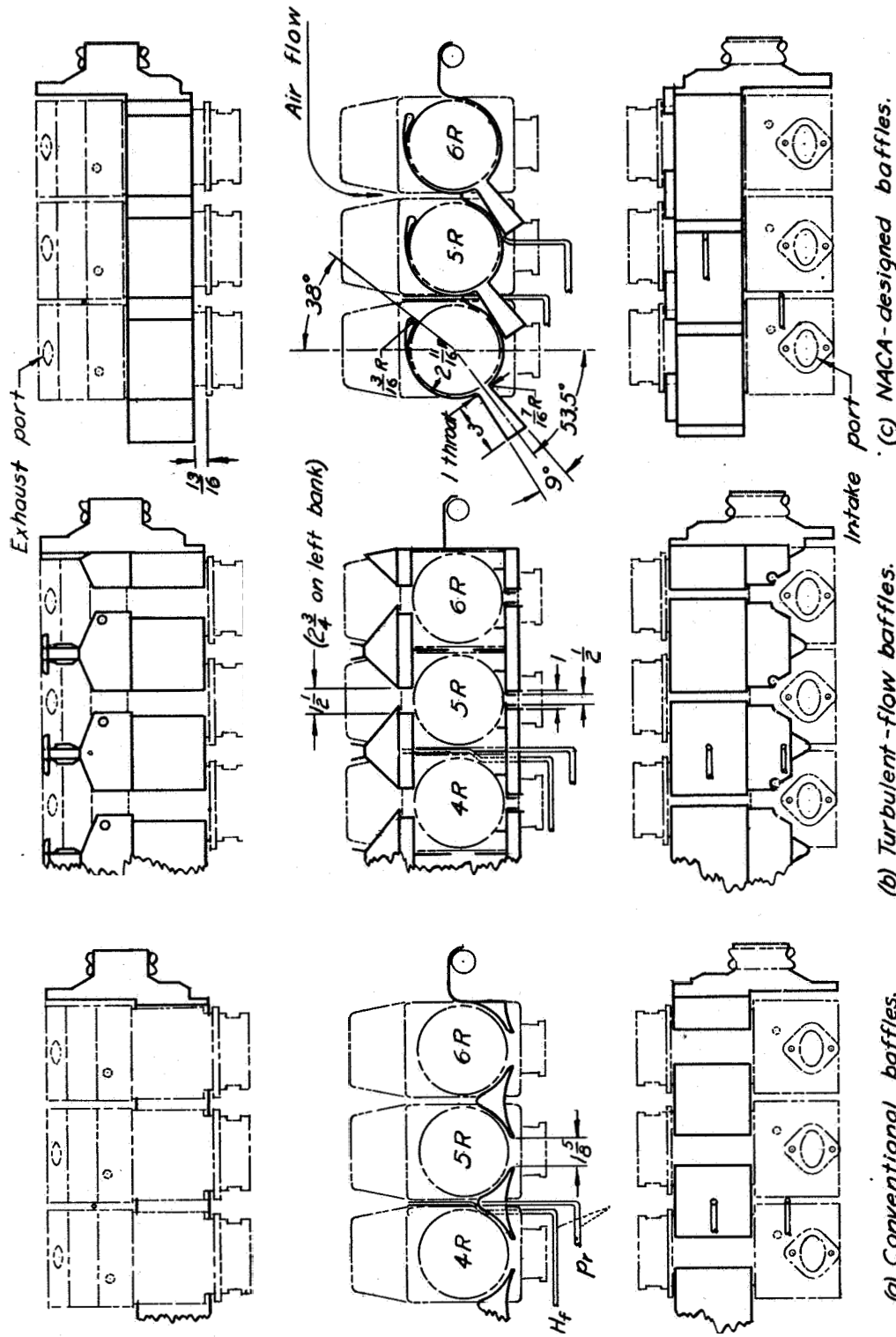


Figure 5.- Engine installation, cowling removed.



NATIONAL ADVISORY  
COMMITTEE FOR AERONAUTICS

Figure 6 . - Typical baffle and pressure tube installations.



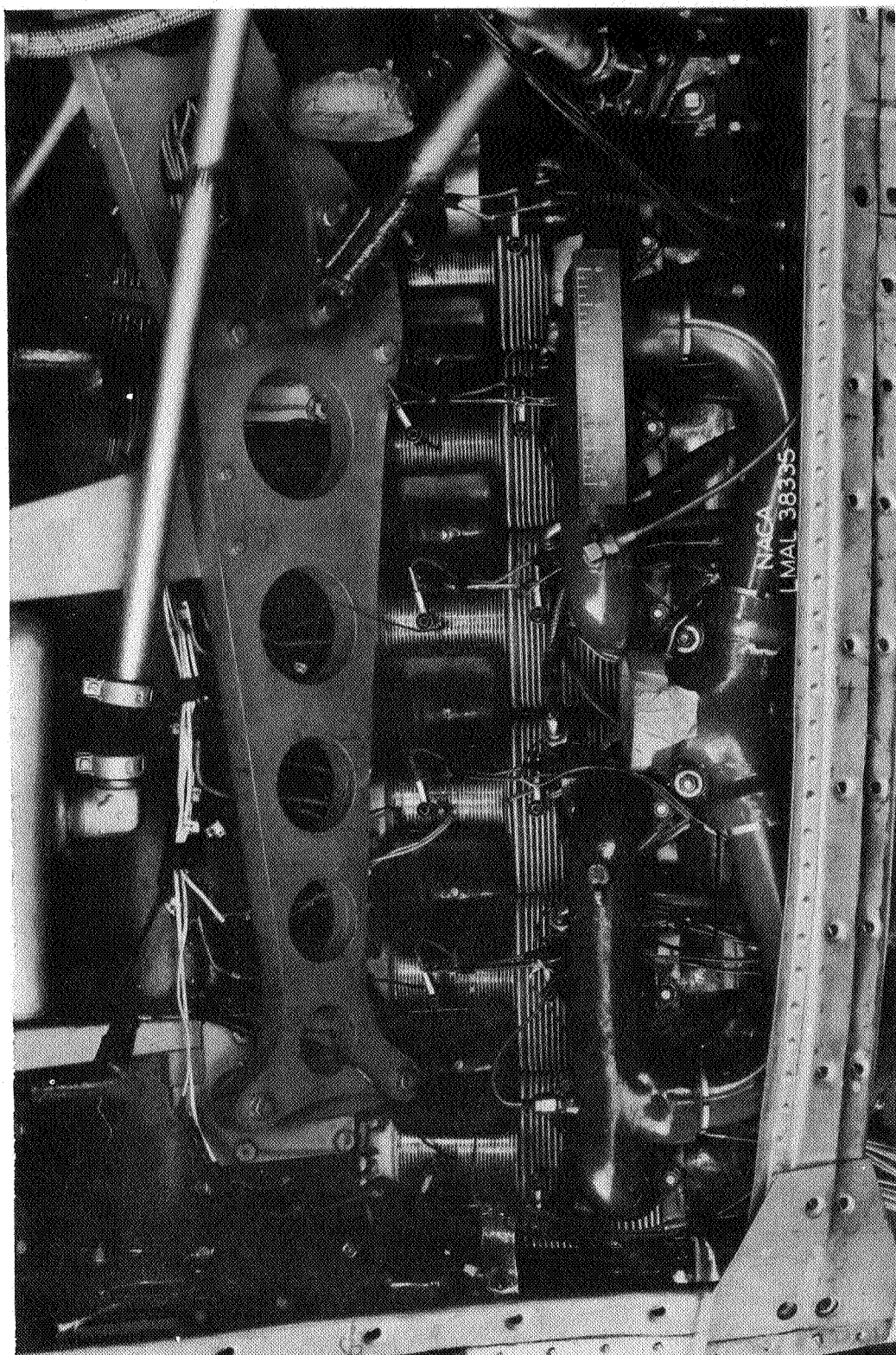
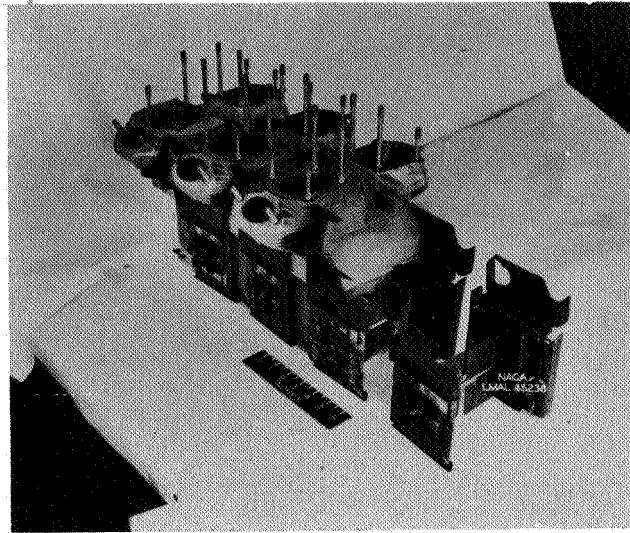
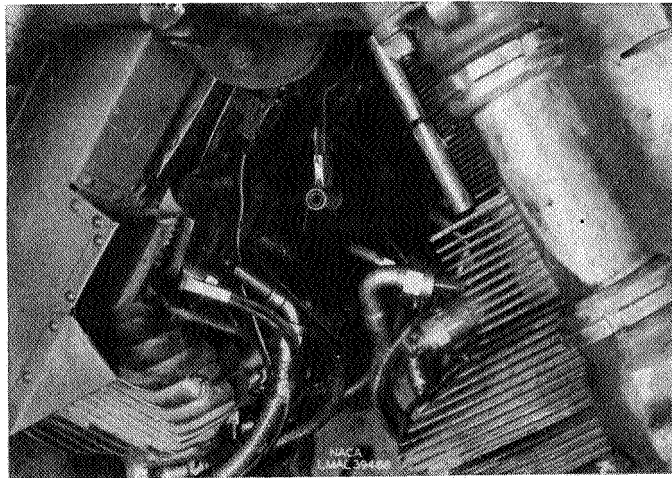


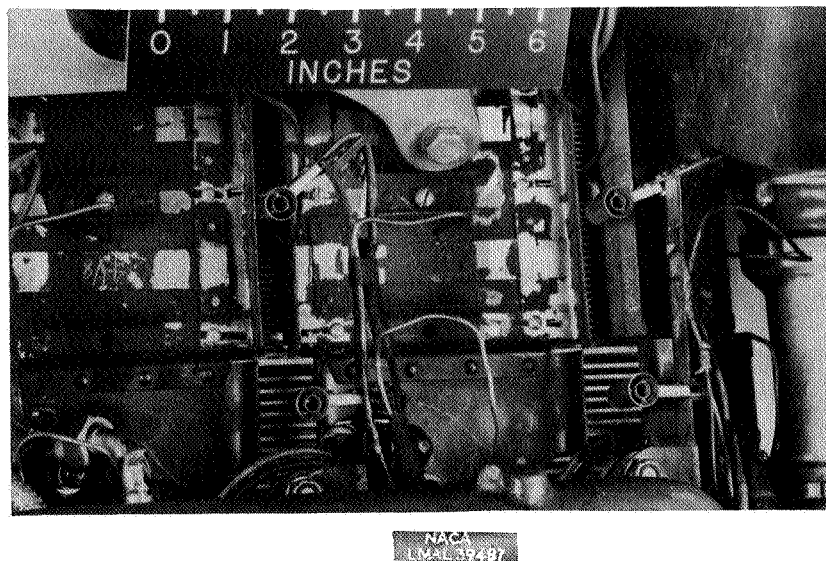
Figure 7.- Installation of conventional baffles.



(a) General arrangement.

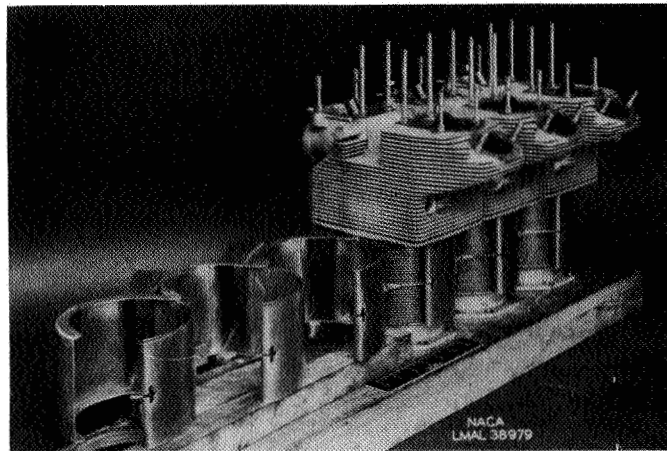


(b) Inboard.

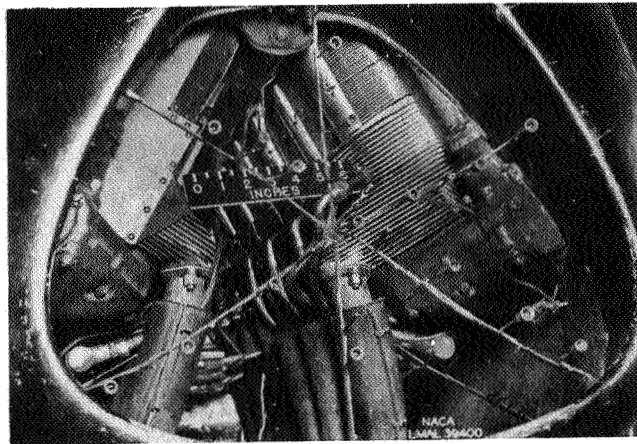


(c) Outboard.

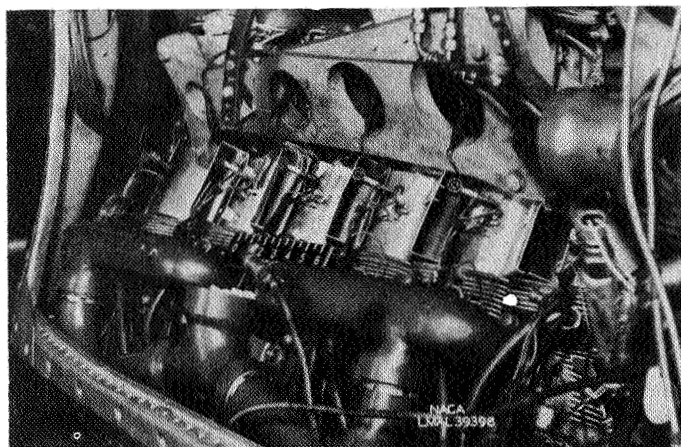
Figure 8.- Installation of turbulent flow baffles.



(a) General arrangement.



(b) Inboard.



(c) Outboard.

Figure 9.- Installation of **diffuser** baffles.

L-561



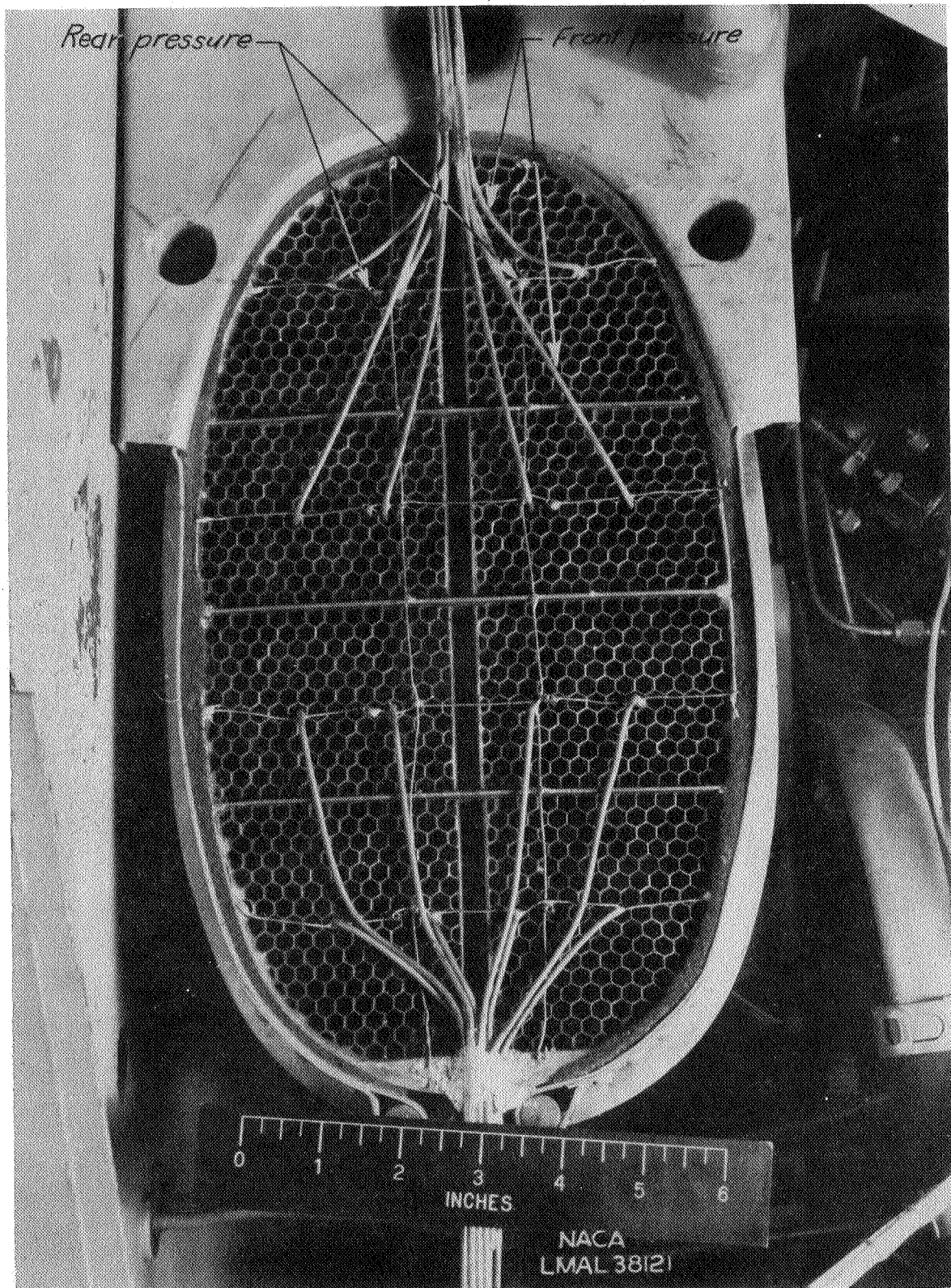


Figure 10.- View of oil-cooler rear face.

MR No. L5112

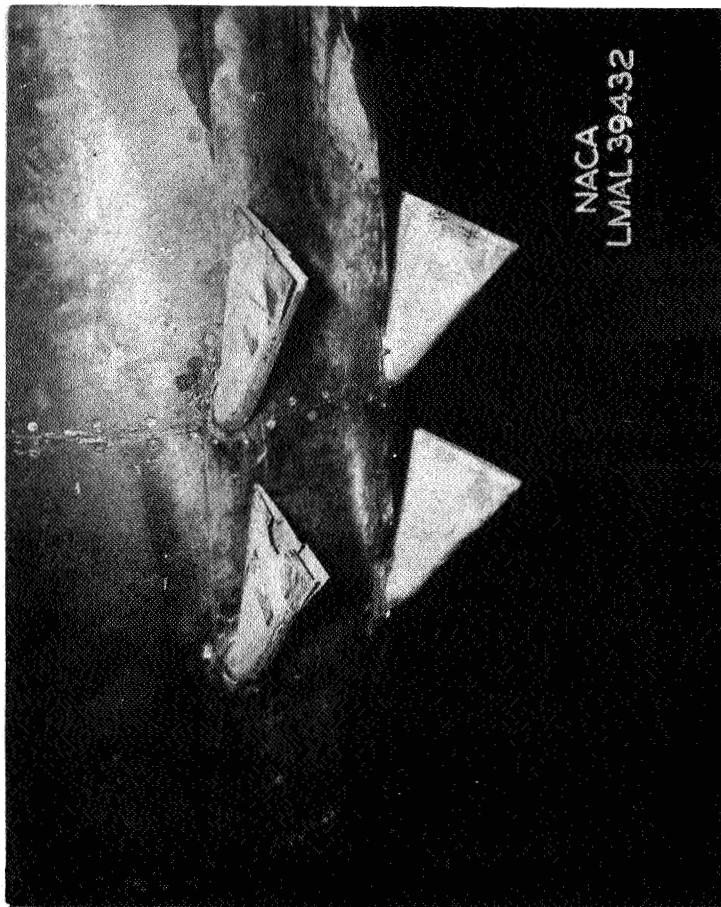
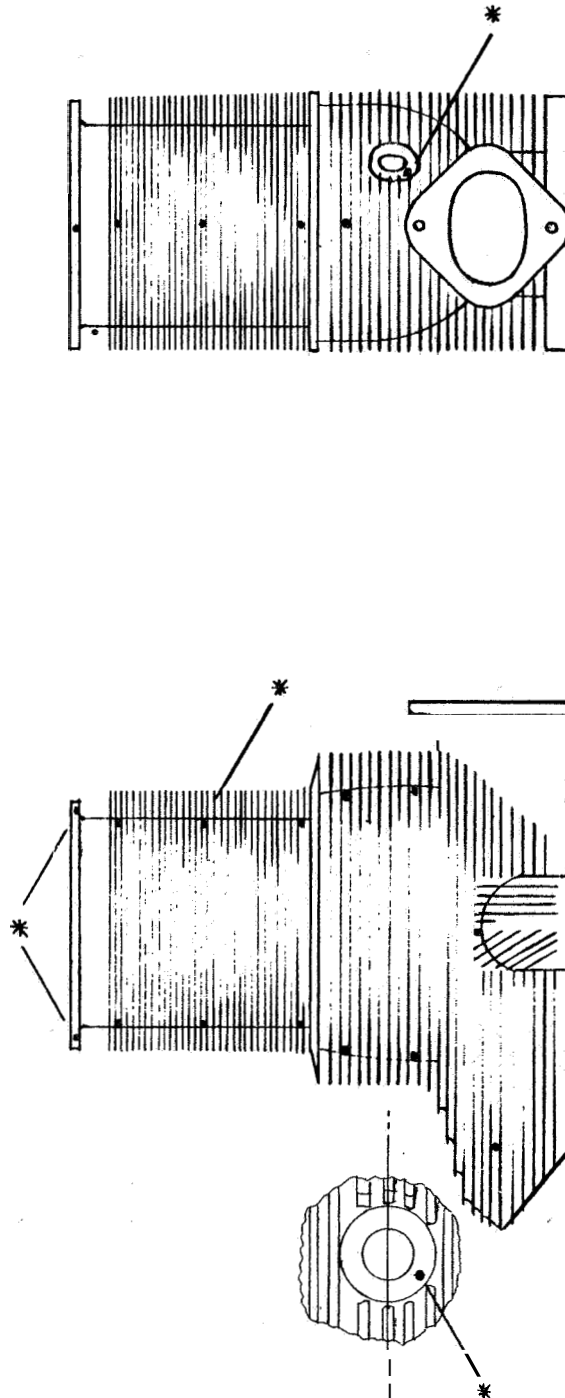


Figure 11. - Vertical flame-damping exhaust stacks  
which failed in operation.

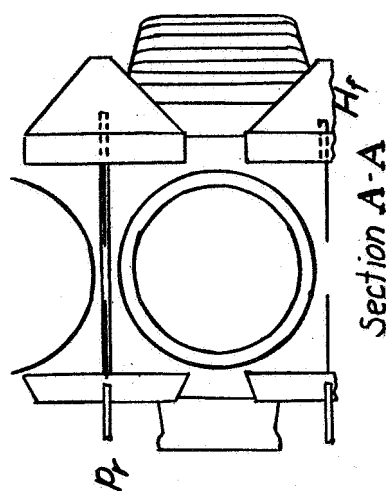


NATIONAL ADVISORY  
COMMITTEE FOR AERONAUTICS

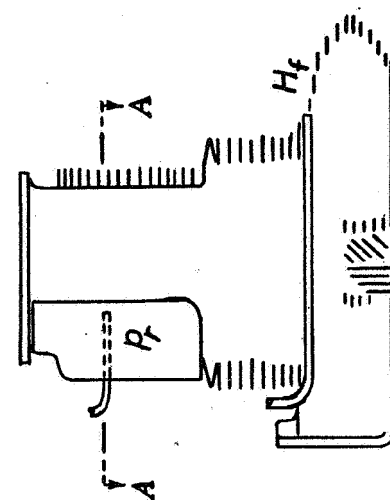


\* Installed on all cylinders. Additional thermocouples shown were installed on 4-L and 4-R only.

Figure 12.- Installation of imbedded thermocouples on the cylinders.



$$\Delta P_e = H_f - P_r$$

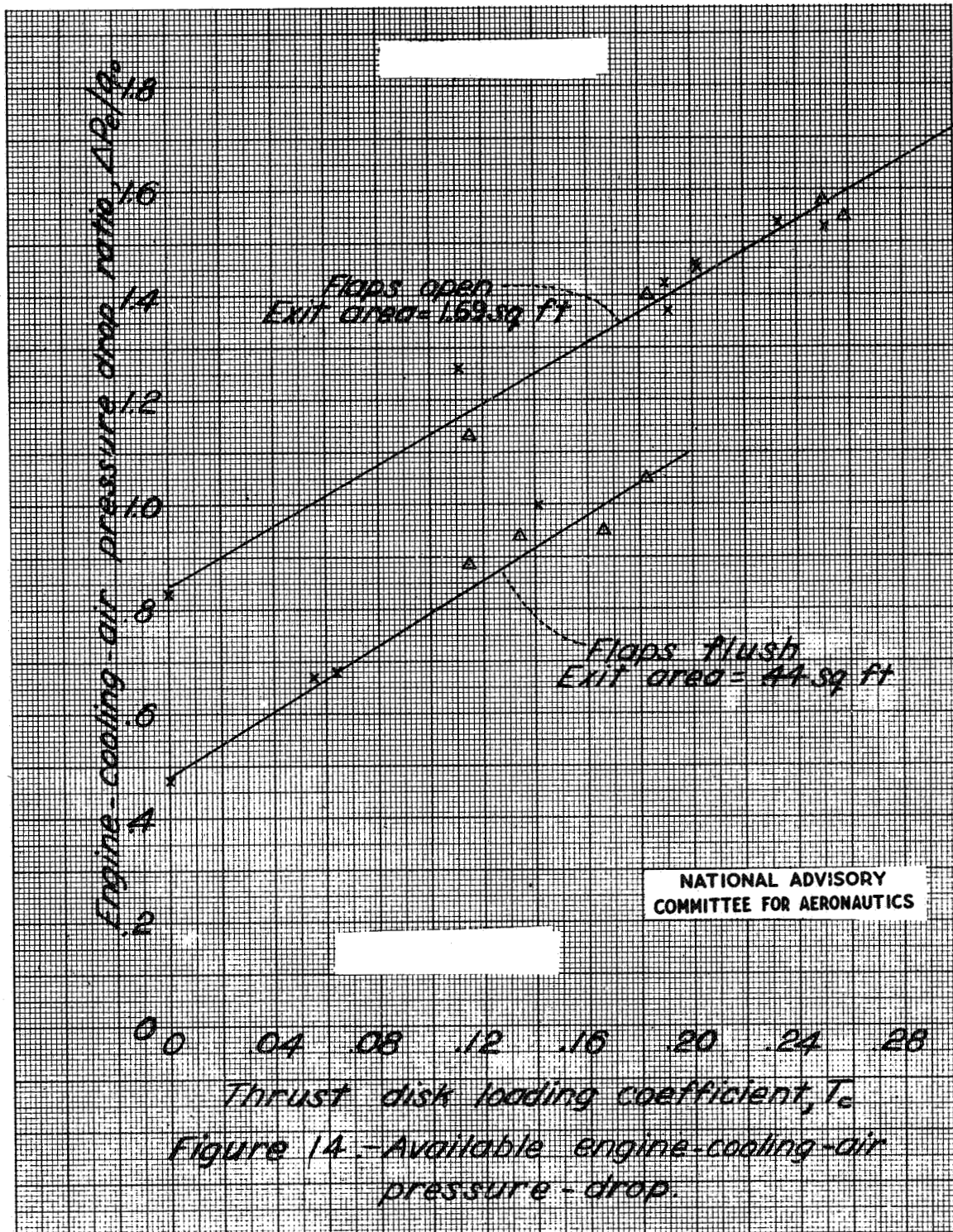


(a) Conventional baffle.

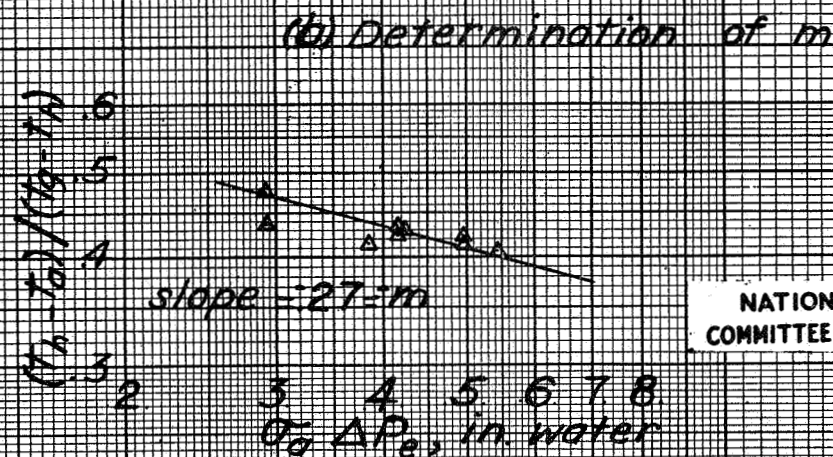
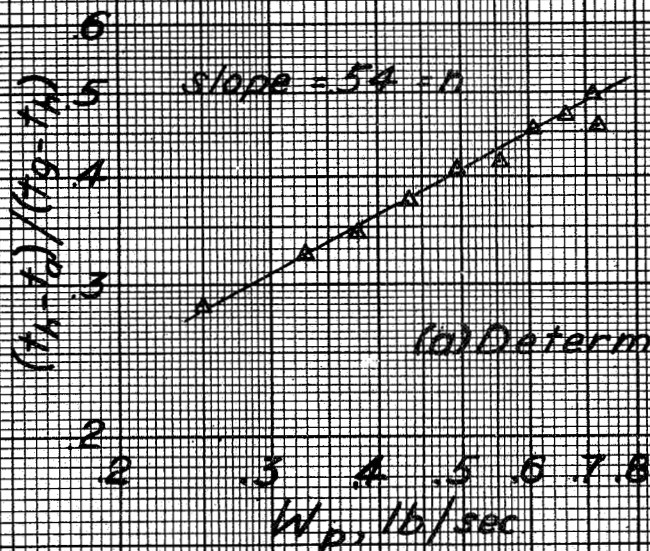
(b) Turbulent-flow baffle.

NATIONAL ADVISORY  
COMMITTEE FOR AERONAUTICS

Figure 13.- Installation of engine-pressure tubes.



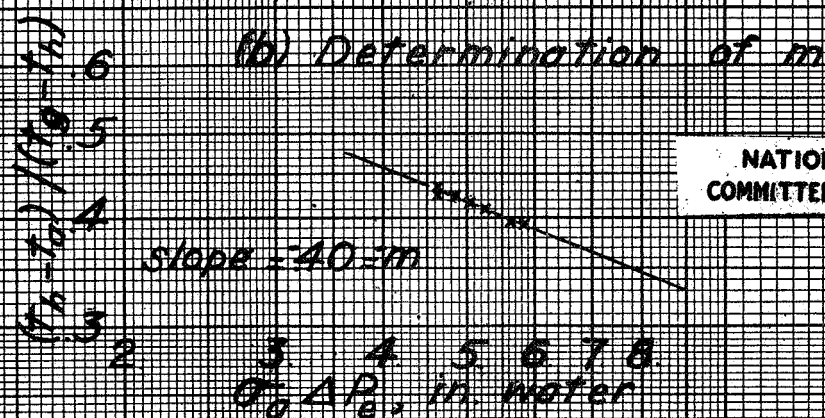
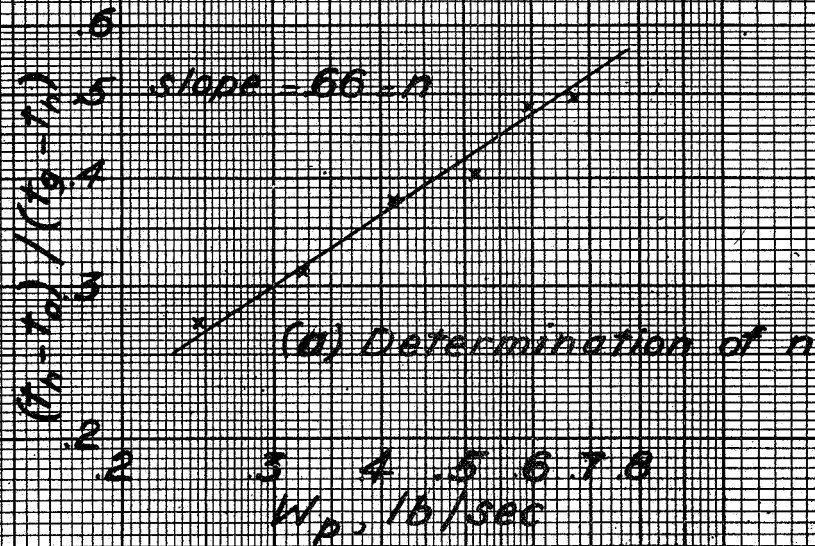




NATIONAL ADVISORY  
COMMITTEE FOR AERONAUTICS

Figure 12. — Construction curves for the engine-cooling-correlation analysis based on average imbedded head temperature. Conventional baffles, configuration II<sub>c</sub>.

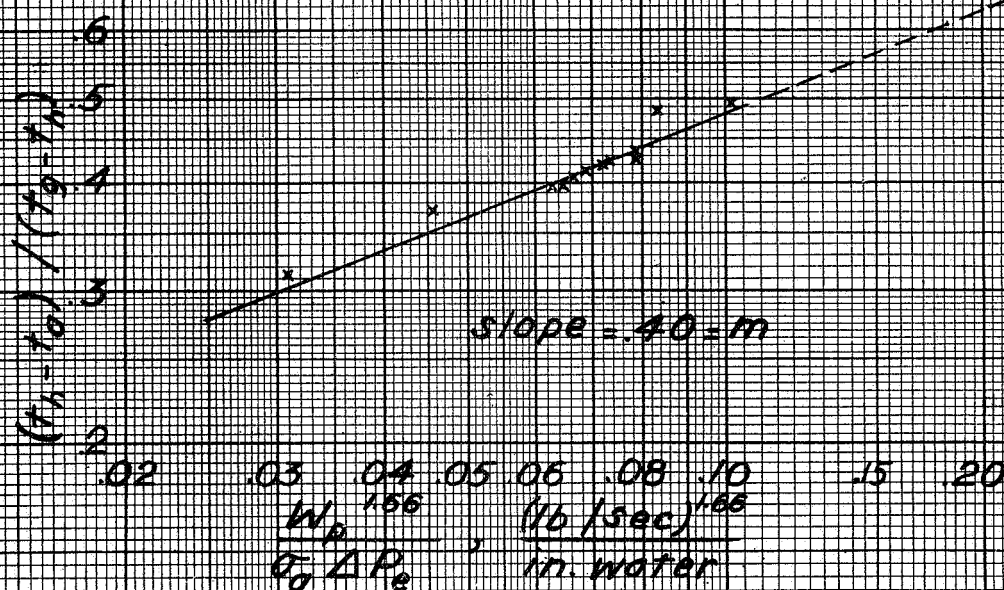
L-561



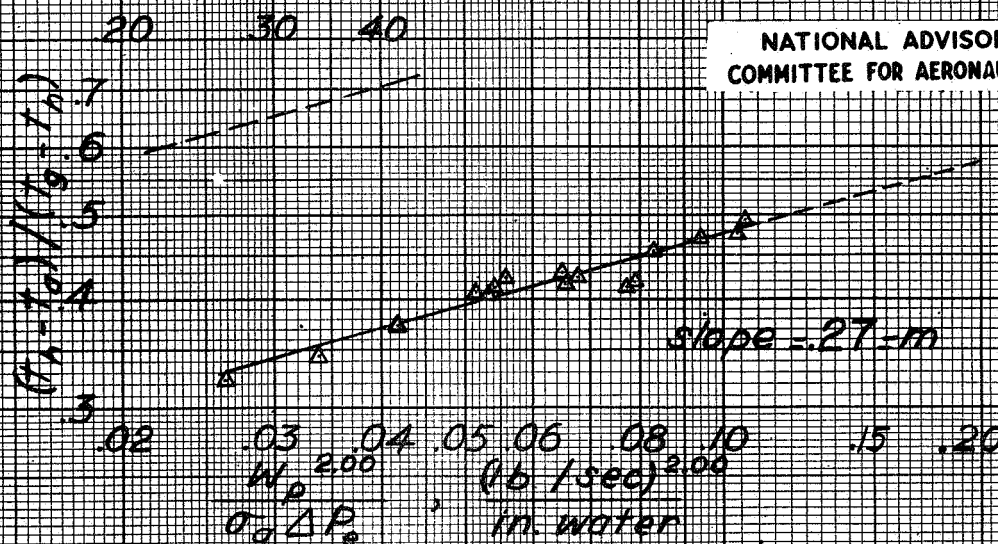
NATIONAL ADVISORY  
COMMITTEE FOR AERONAUTICS

Figure 18 - Construction curves for the engine-cooling-correlation analysis based on average imbedded head temperature. Turbulent-flow baffles, configuration III<sub>0</sub>.



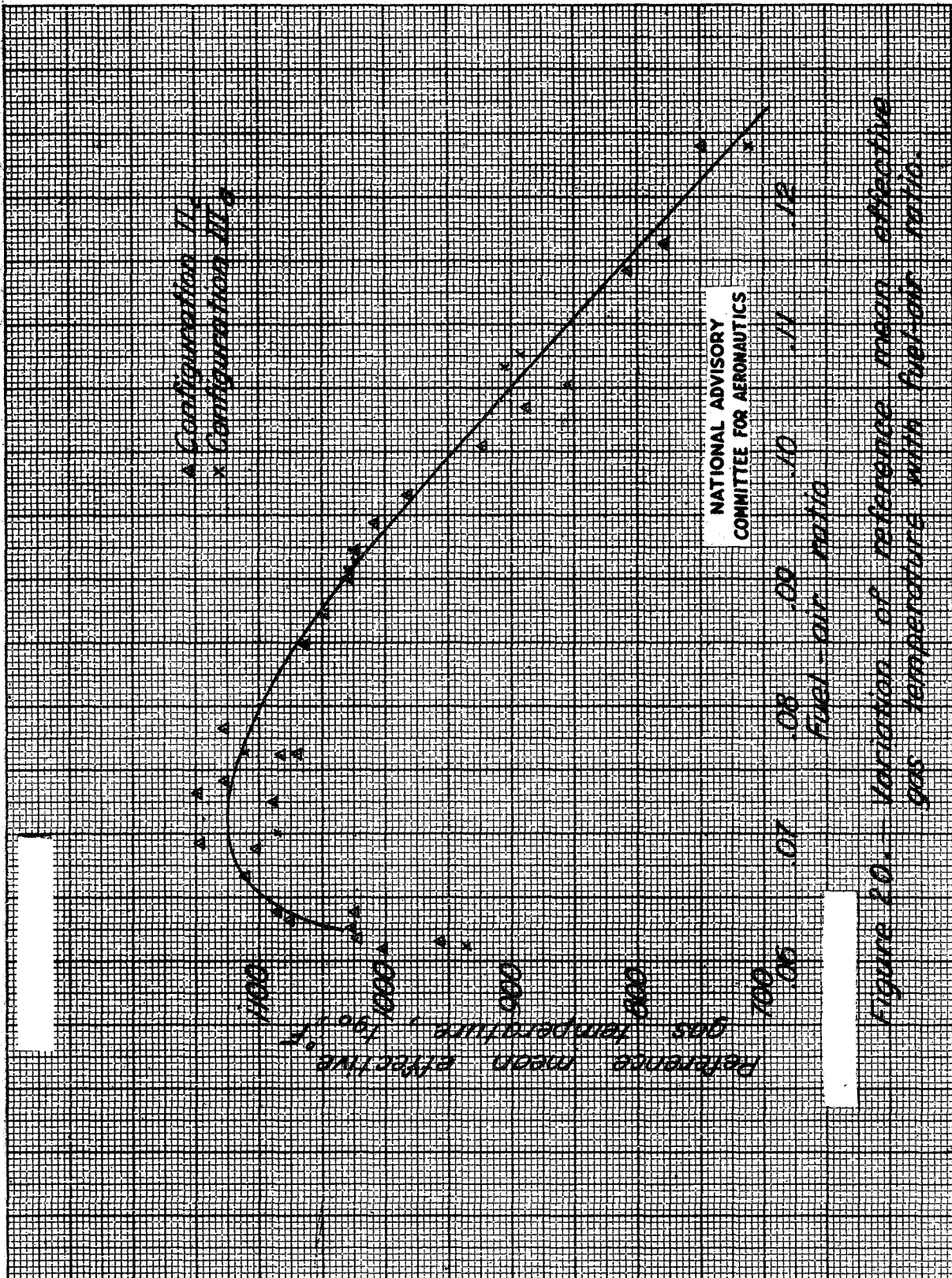


(a) Turbulent-flow baffles, configuration IIIa

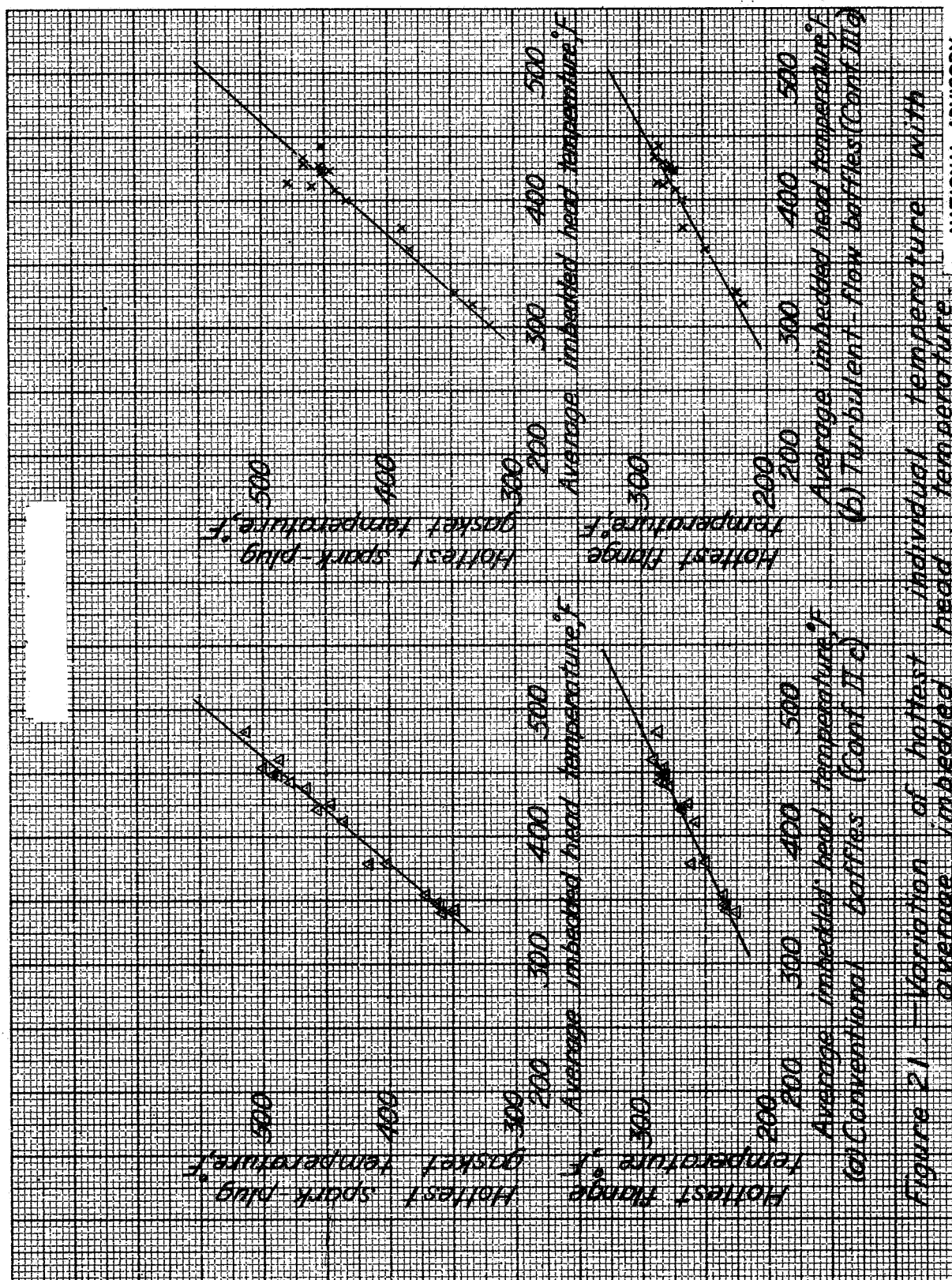


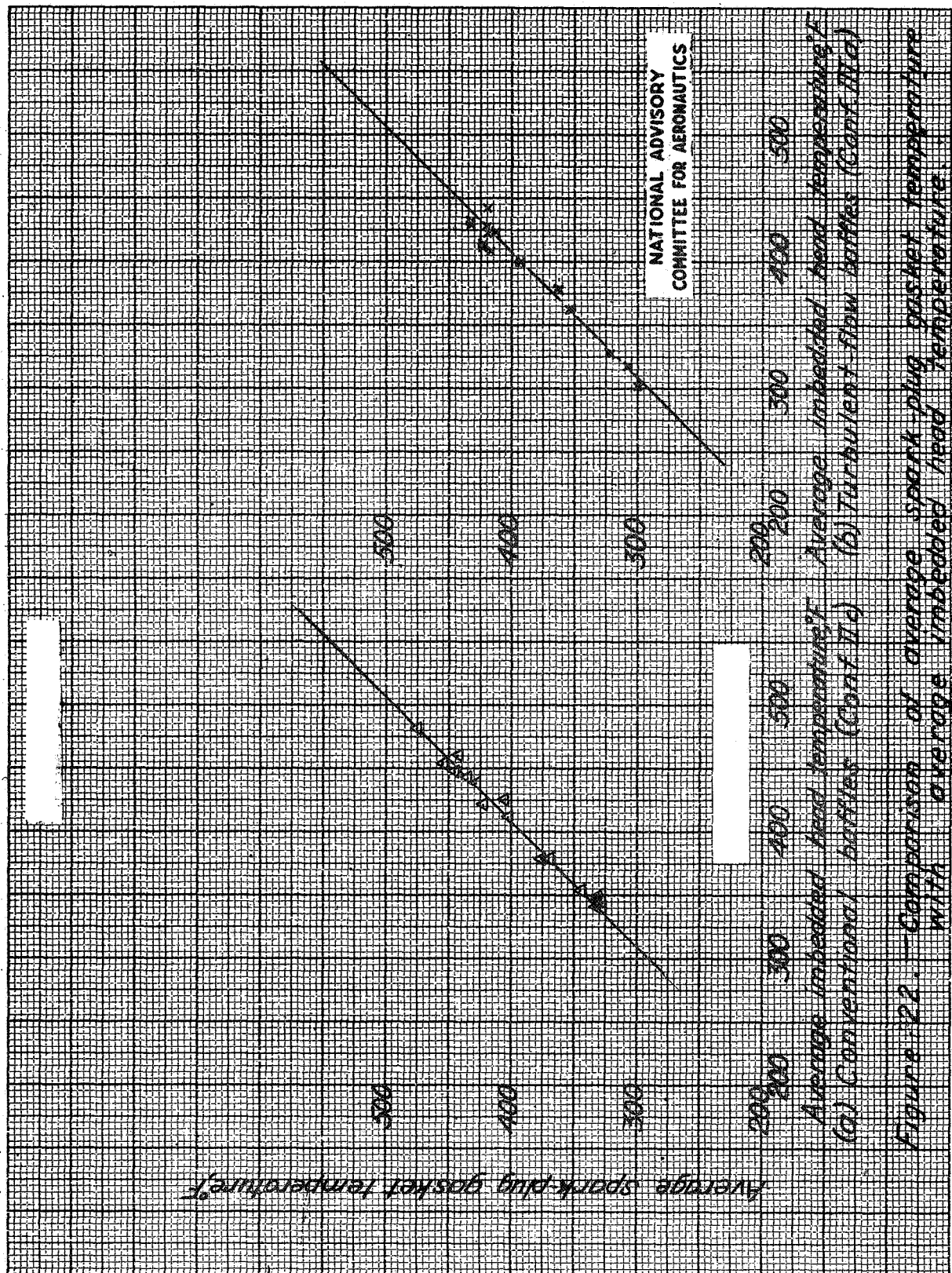
(b) Conventional baffles, configuration IIc

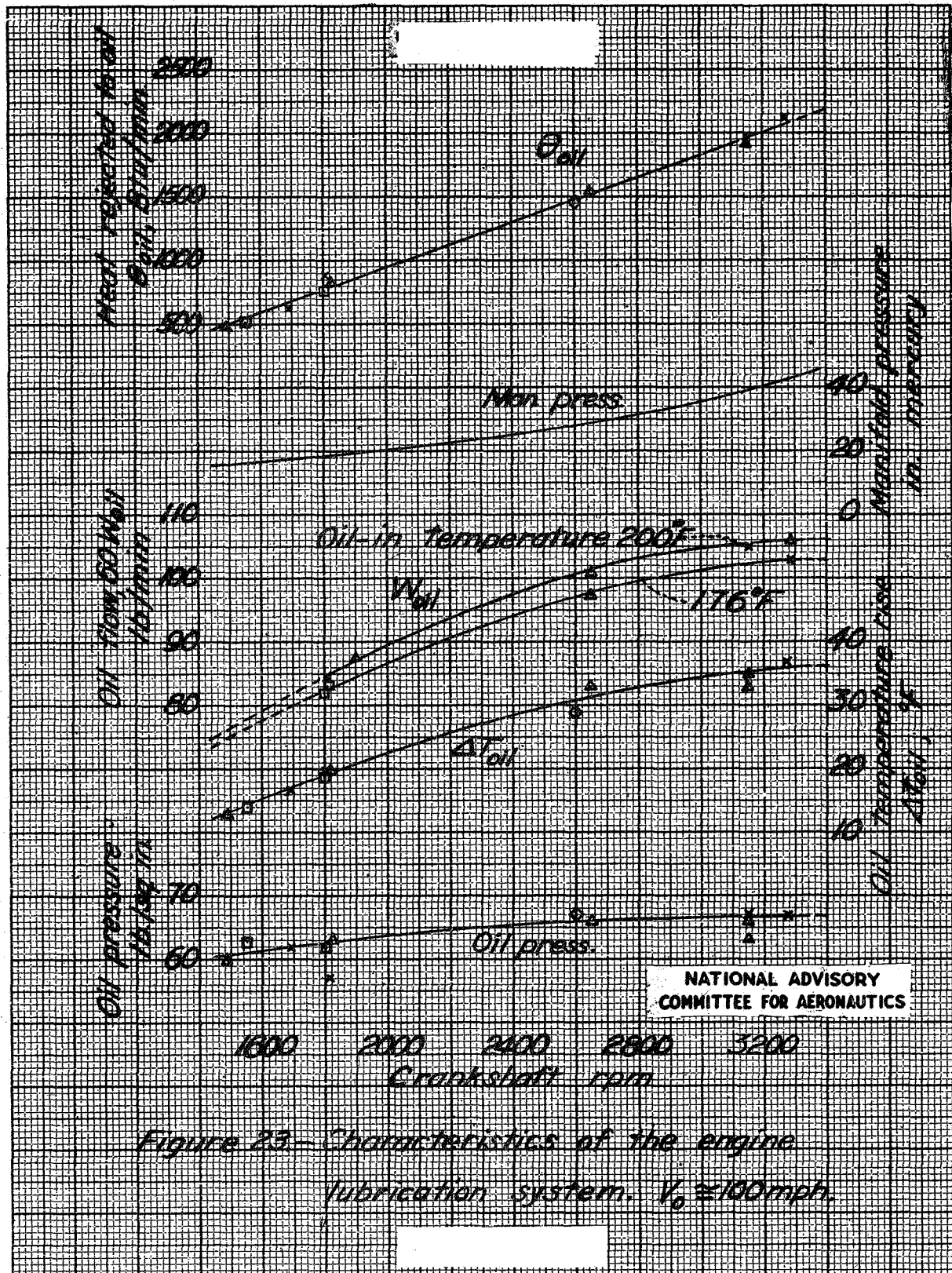
Figure 19. — Engine-cooling-correlation based on average imbedded head temperature.













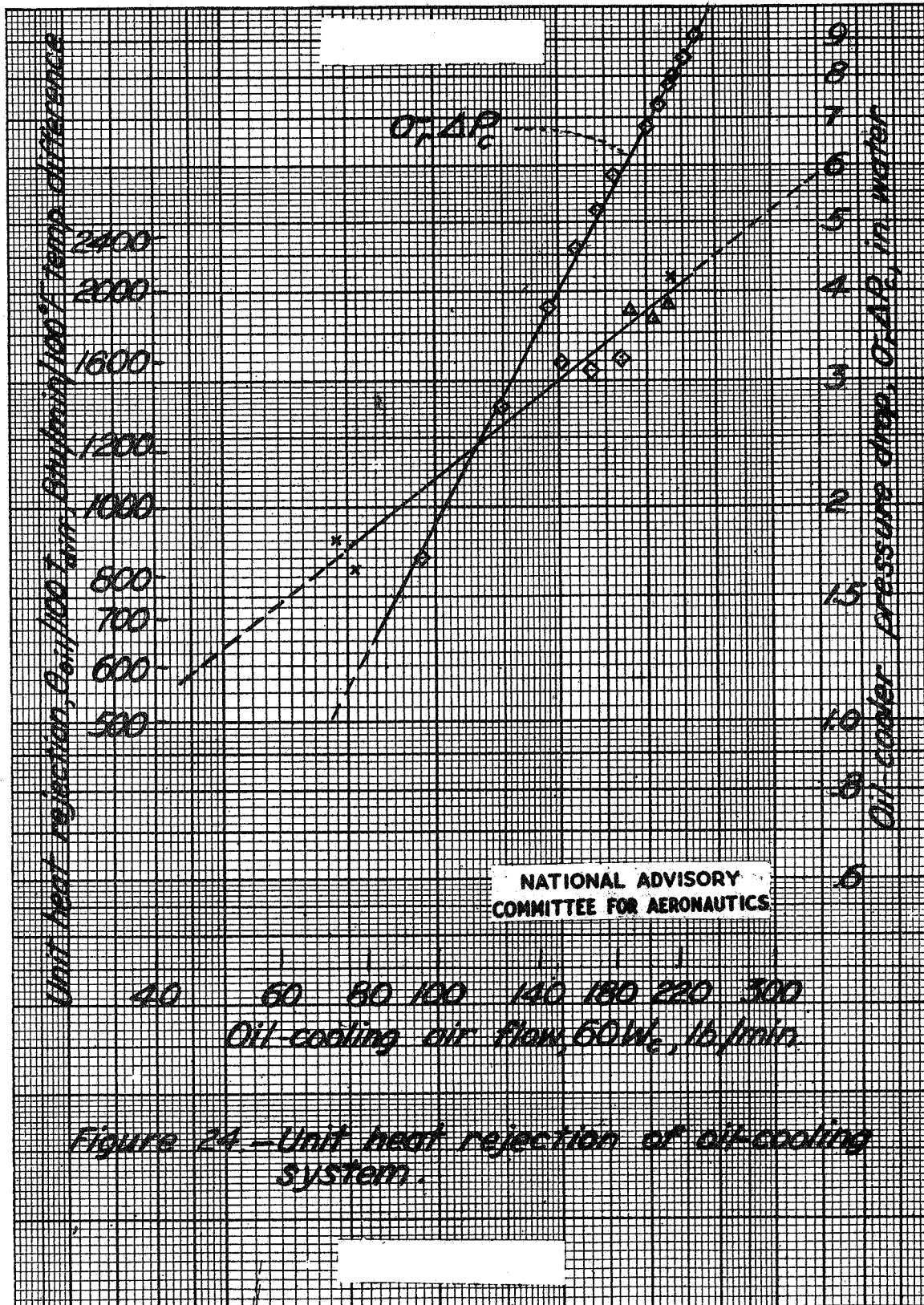


Figure 24 - Unit heat rejection of oil-cooling system.

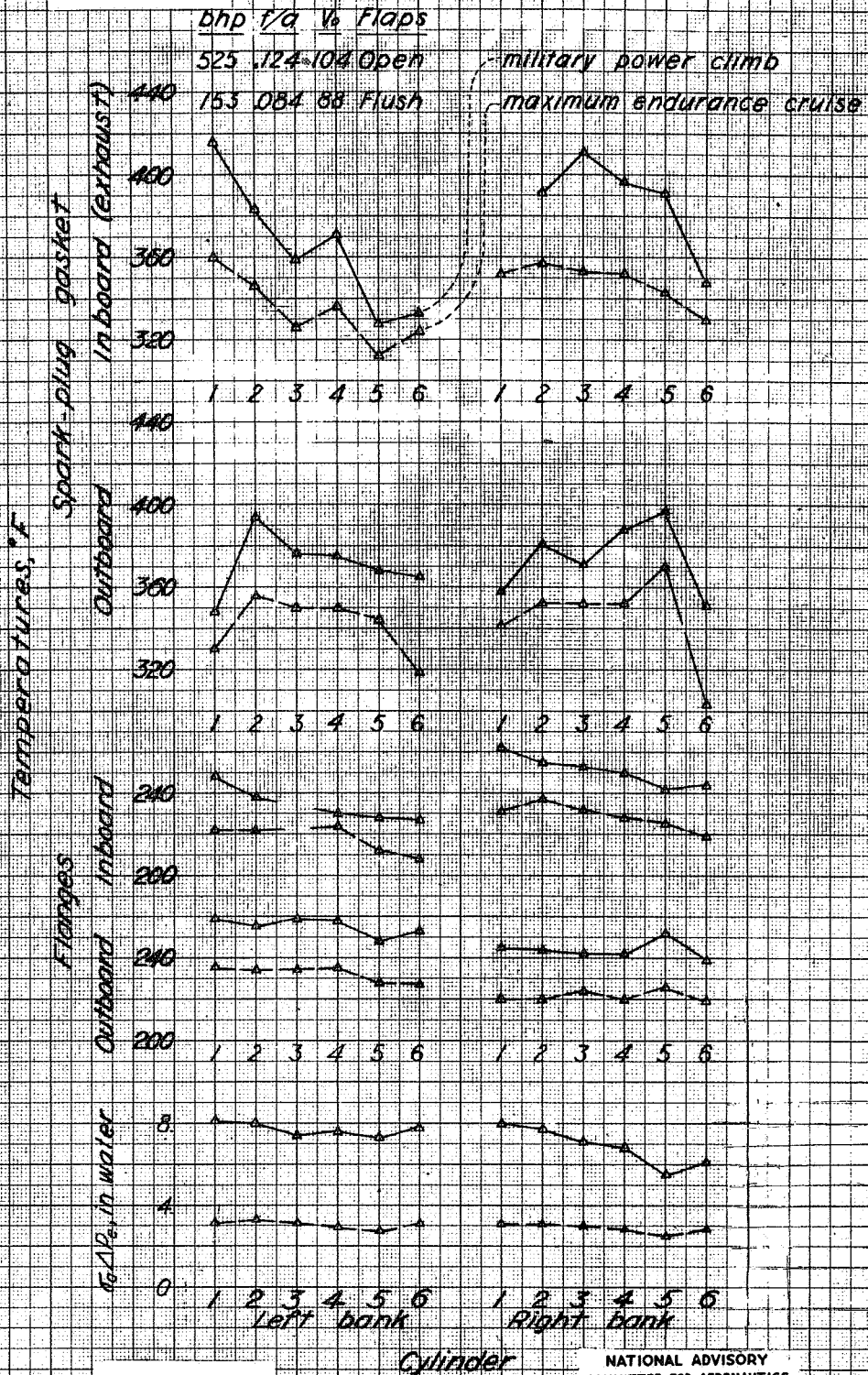
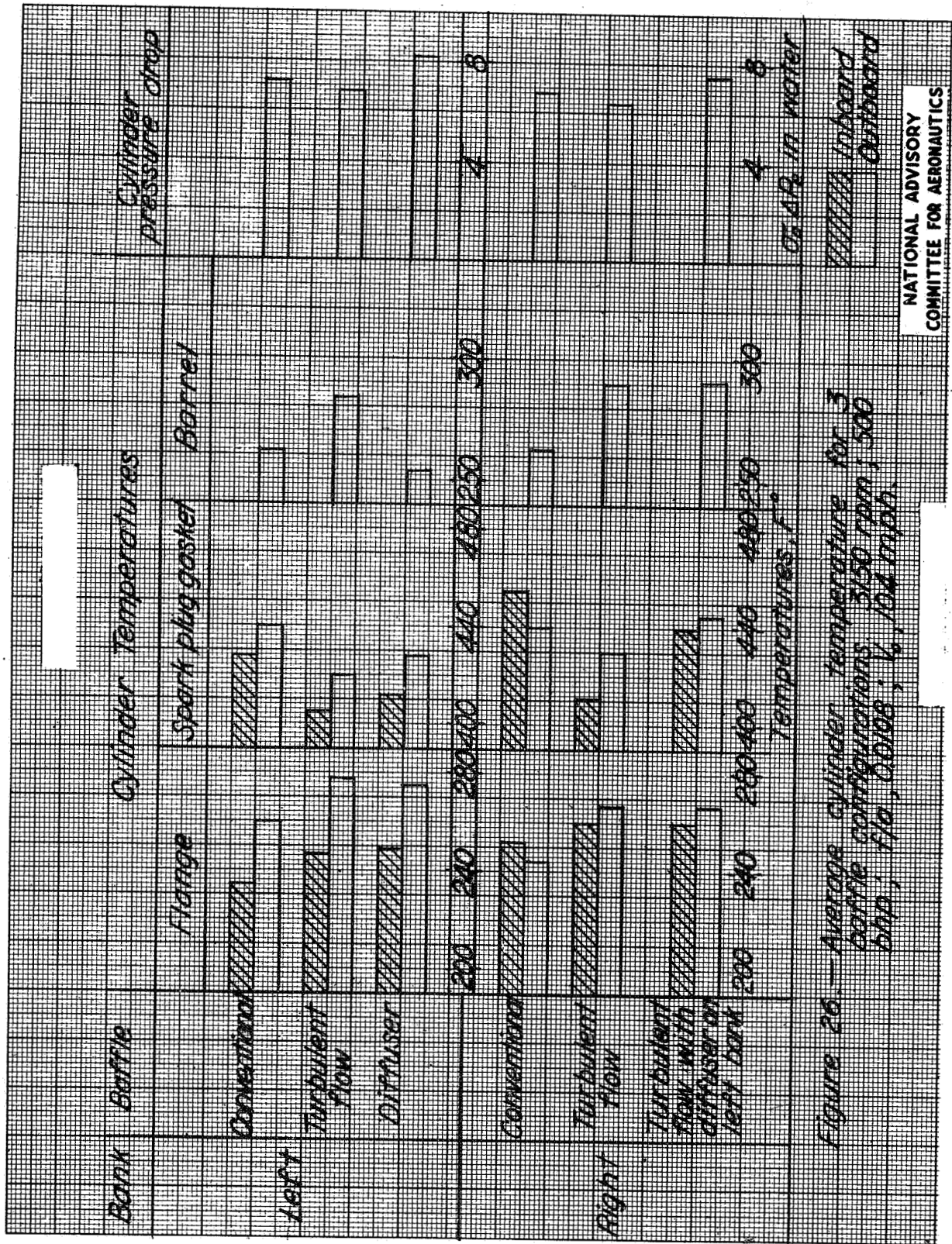


Figure 25.-Engine temperatures in maximum endurance  
cruise and military power climb conditions  
Configuration IIc, conventional baffles



NATIONAL ADVISORY  
COMMITTEE FOR AERONAUTICS





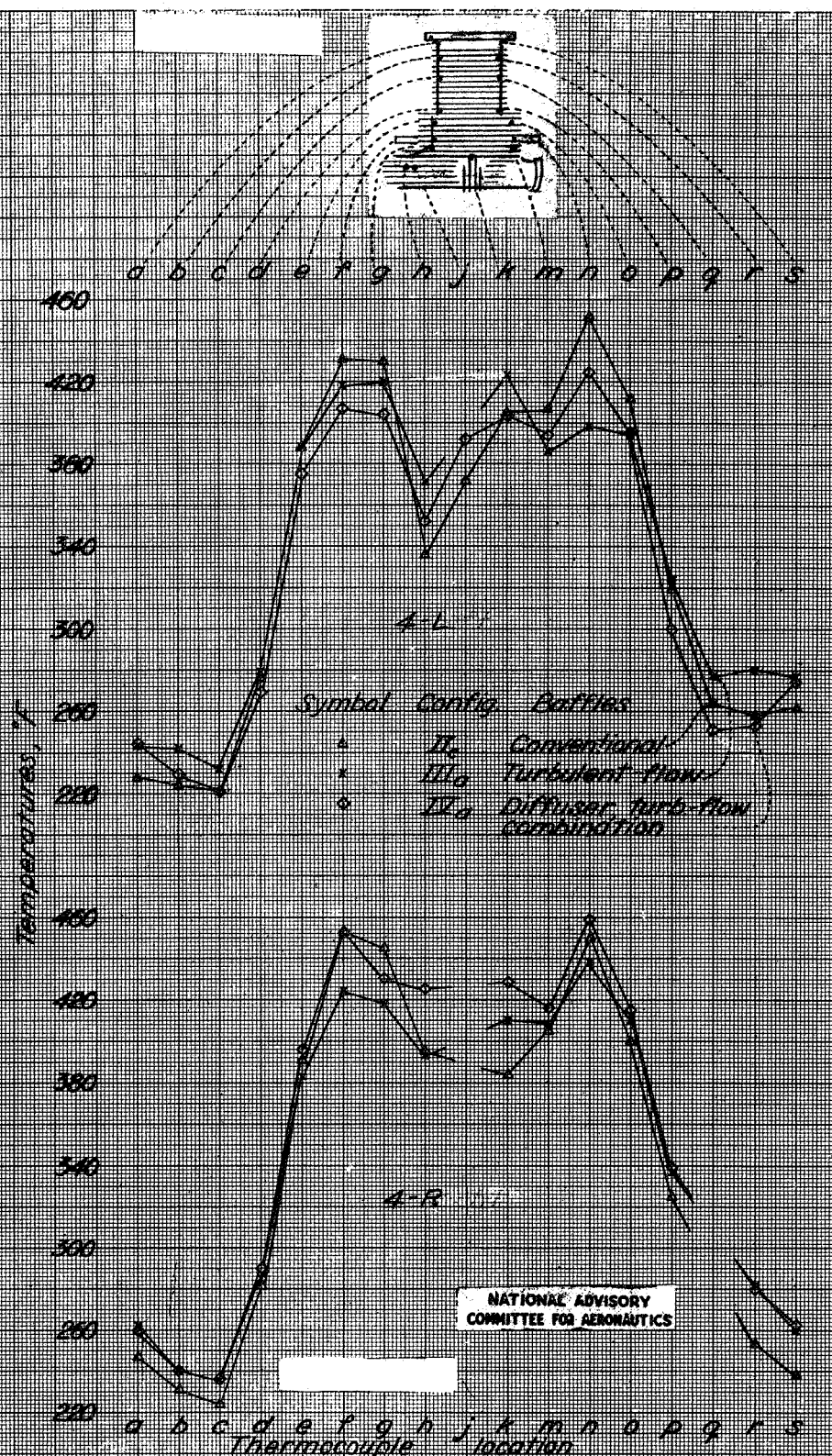


Figure 27 - Concluded.





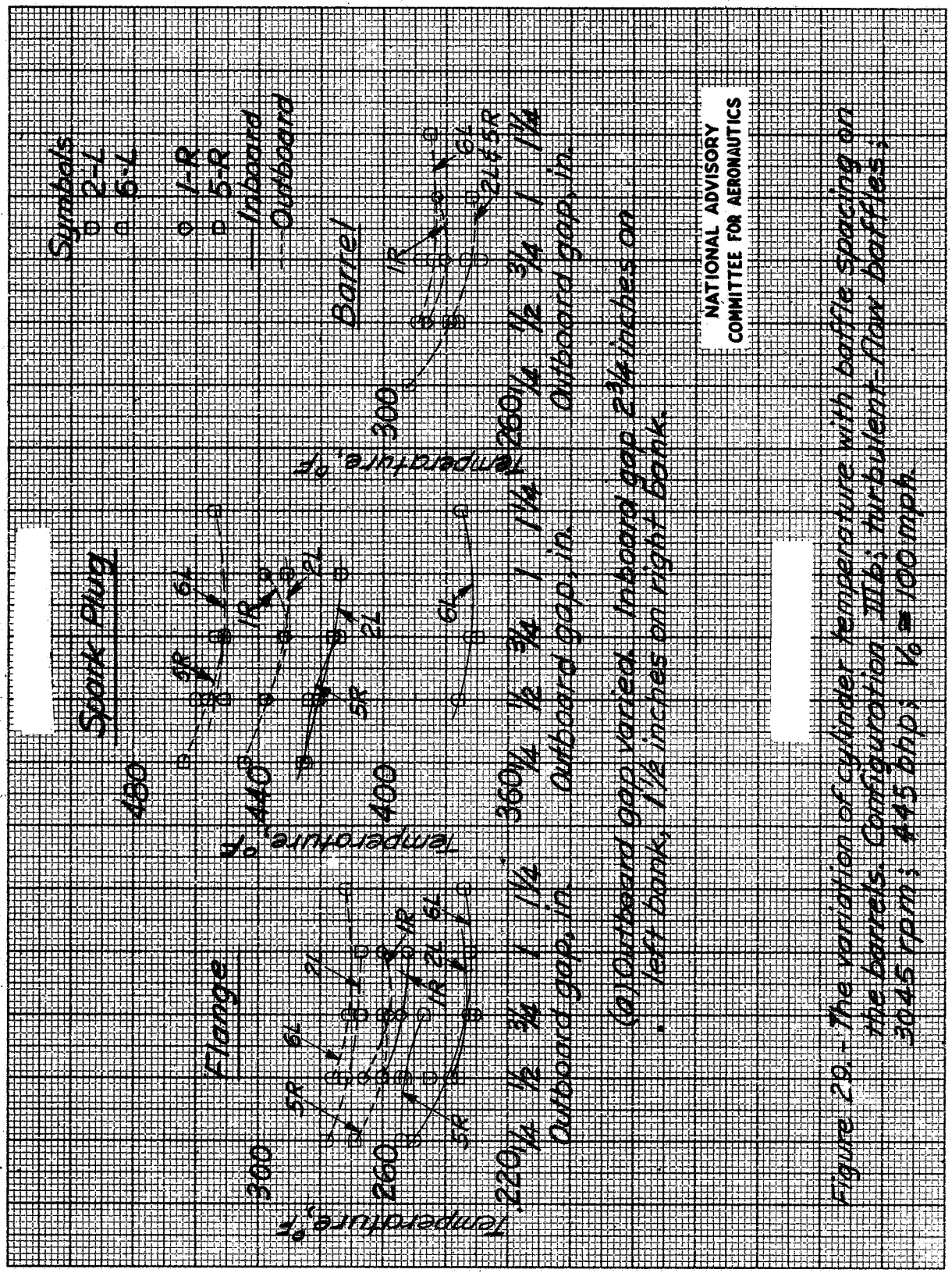
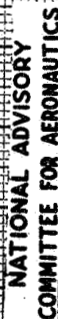


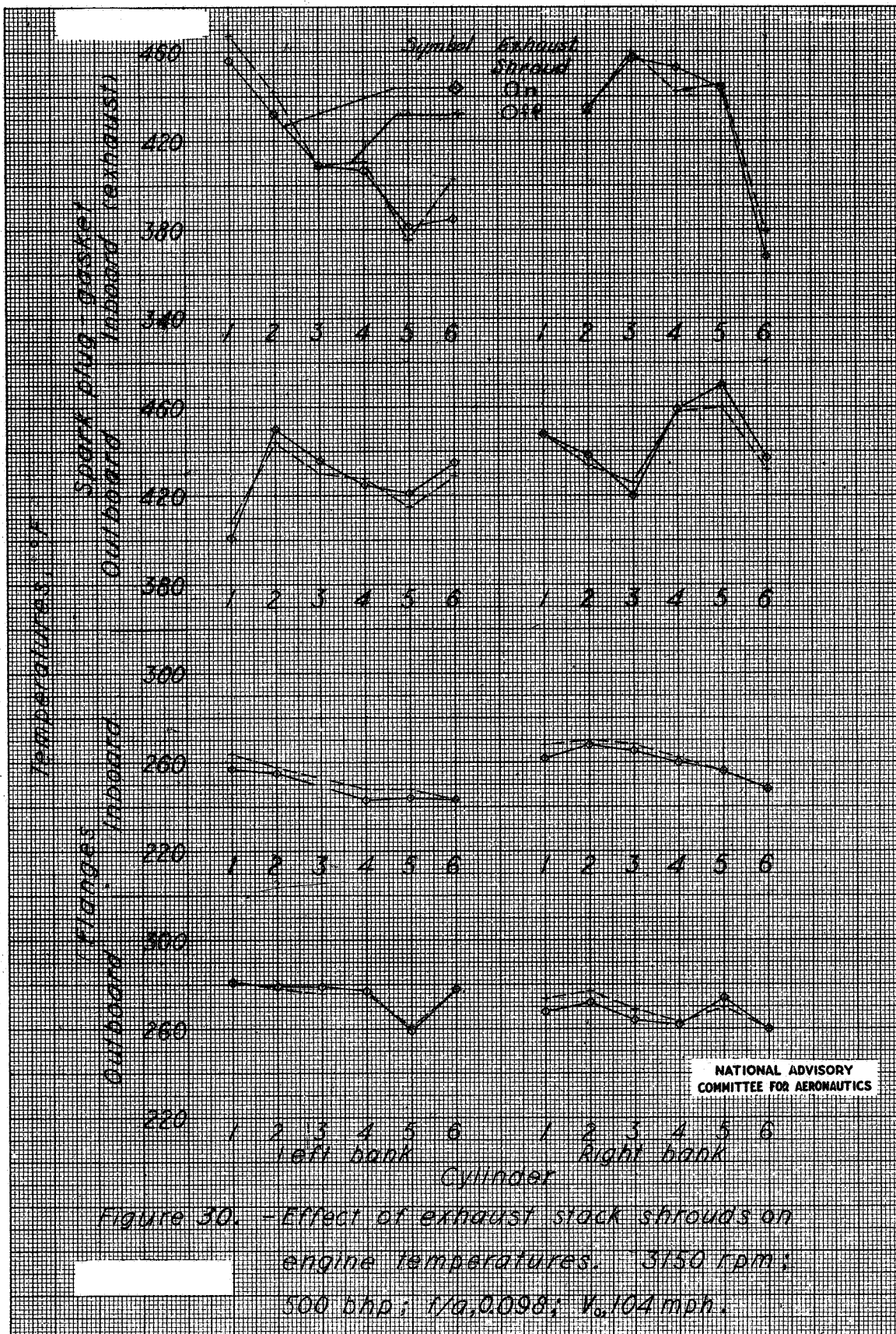
Figure 29 - The variation of cylinder temperature with baffle spacing on the barrels. Configuration IIIb; turbulent-flow baffles; 3045 rpm; 445 bhp;  $V_0 = 100$  mph.





(c) Inboard prop varied.

**Figure 29. — Concluded**





L-561

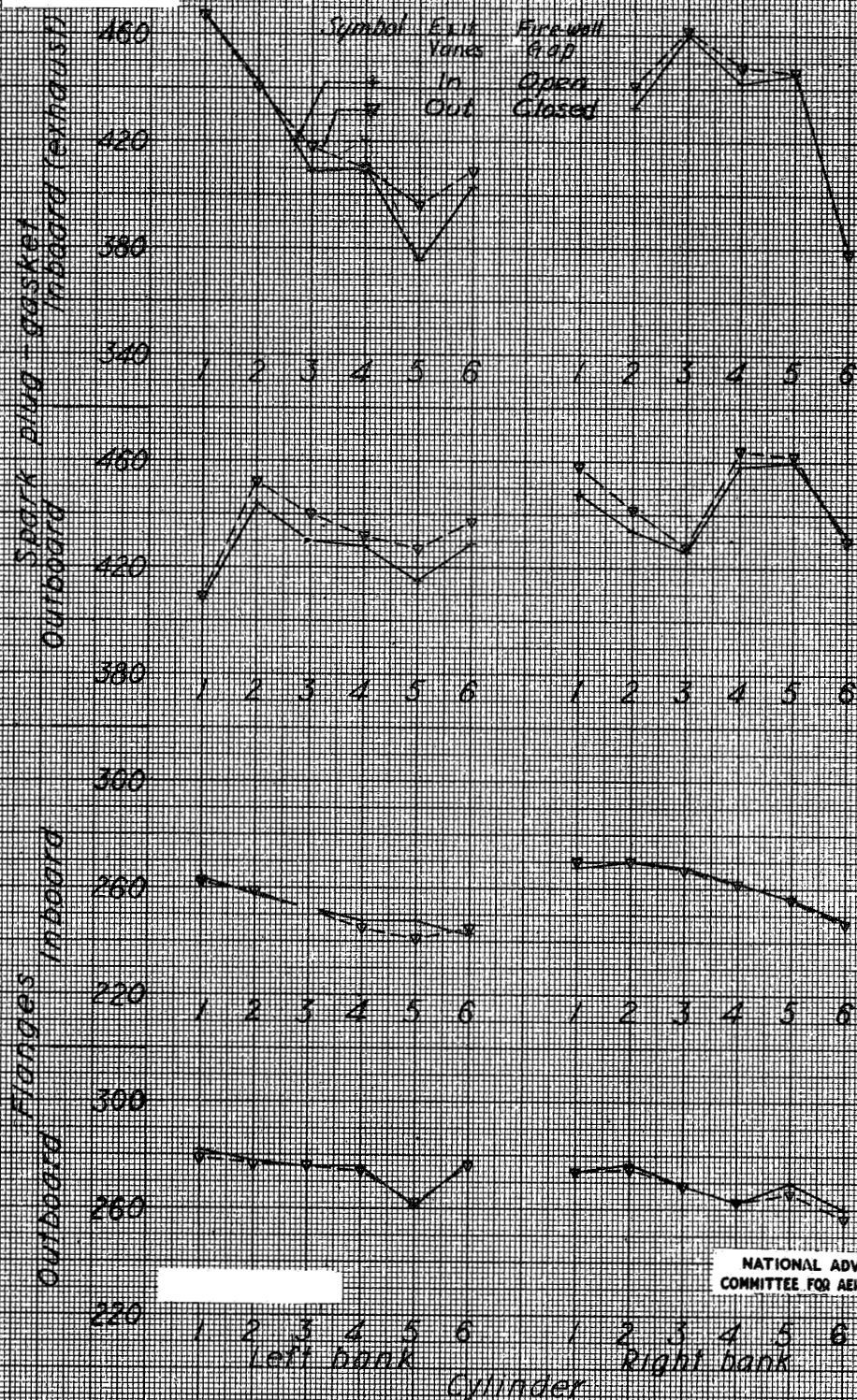


Figure 36-Effect of firewall gap and engine air exit vanes on engine temperature. Exhaust shrouds removed; 3150 rpm; 500 bhp;  $t/a$ , 0.098;  $V_a$ , 104 mph.